
Decision-Focused On-Policy Learning for Contextual Linear Optimization with Partial Feedback

Wyame Benslimane^{*,1}, Tinghan Ye^{*,2}, Pascal Van Hentenryck², Paul Grigas¹

¹Department of Industrial Engineering and Operations Research
University of California, Berkeley
{wyame.benslimane, pgrigas}@berkeley.edu

²H. Milton Stewart School of Industrial and Systems Engineering
Georgia Institute of Technology
{joe.ye, pvh}@gatech.edu

*Equal contribution.

Abstract

Decision-focused learning (DFL) trains predictive models by optimizing downstream decision quality rather than standalone prediction accuracy. For contextual linear optimization, most existing DFL methods assume offline data and full observations of the objective cost vector. We develop an on-policy learning method for sequential contextual linear optimization under partial feedback, generalizing the standard bandit feedback setting. Our method learns a stochastic predict-then-optimize policy that samples a cost-vector prediction from a conditional distribution and solves the resulting downstream linear optimization problem. To update this distributional model, we introduce a two-component hybrid gradient estimator. The first component is a score function estimator, which provides an unbiased but potentially high-variance policy gradient estimate. The second is a decision-focused plug-in component that uses an auxiliary nuisance estimate of the latent cost vector to exploit the downstream optimization structure, becoming more informative as the estimate improves. We prove an $\mathcal{O}(T^{-1/2})$ bound on the average squared policy-gradient norm, matching the standard non-convex SGD rate. Experiments on top- k selection, shortest path, combinatorial pricing, and a real-data energy-scheduling benchmark show that the hybrid gradient approach achieves lower cumulative regret than contextual-bandit-style baselines across all benchmarks, using both Gaussian and richer conditional generative models. Code is available at <https://github.com/Joeyetinghan/on-policy-bandit-dfl>.

1 Introduction

Many operational systems make sequential decisions by solving constrained optimization problems given observed contextual information, with applications spanning vehicle routing, dynamic pricing, power scheduling, product allocation, and recommendation (Van Hentenryck and Bent, 2006; Powell, 2022; Elmachtoub and Grigas, 2022; Li et al., 2010; Zhao et al., 2026; Sadana et al., 2025). In these settings, the feasible set and operational constraints are known, while the relevant cost or reward parameters are uncertain at decision time and instead must be learned. When such systems are deployed repeatedly, the learner is not merely trained on a fixed historical dataset; its own decisions become part of the data-generating process, determining which outcomes are observed and hence what information is available for future learning. Furthermore, the collected data rarely include full information about problem parameters: a selected route reveals only the realized travel time, a posted price reveals only demand at that price, a recommended subset reveals only response on the chosen

items. The learner thus repeatedly sees a context, chooses a feasible decision from the current policy, and observes only the feedback generated by that decision. This paper studies sequential contextual linear optimization (CLO), a widely applicable class of constrained optimization problems, in this on-policy decision-making environment with partial feedback.

The combination of constrained optimization and online decision-making with partial feedback is not yet captured systematically by any one existing framework. DFL trains predictions through the decisions they induce (Mandi et al., 2024; Elmachoub and Grigas, 2022), but most existing methods assume batch data and full observations of the latent cost vector in CLO. Contextual bandits and online learning study sequential learning from partial feedback, including large and structured action spaces (Li et al., 2010; Abbasi-Yadkori et al., 2011; Krishnamurthy et al., 2016; Zhu et al., 2022), but typically model rewards directly over context-action pairs rather than preserving and strongly exploiting the downstream linear optimization model. Given the surge of development in powerful DFL methods for offline problems with full data (Mandi et al., 2024), a natural question emerges: can DFL methods be adapted to on-policy, sequential decision-making with partial feedback?

We answer affirmatively by introducing a new class of on-policy stochastic gradient estimators that enables strong plug-in/predict-then-optimize policies. We learn a structured conditional distribution over cost vectors and induce decisions through linear optimization, rather than a direct context-to-decision map. We update the policy parameters by mixing two gradient signals with complementary trade-offs. A score function estimator uses the on-policy realized cost directly, making it unbiased for the induced policy objective and naturally tied to exploration through sampling. However, the score function approach treats the downstream optimizer as a black-box action generator and therefore does not strongly use the structure of the feasible set or linear objective in its gradient. We therefore propose a decision-focused plug-in gradient estimator that leverages linear optimization structure by pairing the known feasible set with a nuisance estimate, adapted from the offline/off-policy case (Hu et al., 2024b, 2025), of the conditional mean cost vector. Once the nuisance estimate is plugged-in to a cost approximation, the resulting problem is equivalent to a full information contextual stochastic linear optimization problem and can be tackled with all of the machinery, such as surrogate loss functions, developed in recent years (Mandi et al., 2024; Sadana et al., 2025). We bound the bias of this nuisance estimator approach and show its advantages grow as data accumulates.

Contributions. *First*, we develop an on-policy decision-focused learning method for online contextual linear optimization under a generic partial-feedback model that subsumes bandit, semi-bandit, and full-information settings. The policy update is a hybrid gradient combining an unbiased score function term with a decision-focused plug-in term from a learned auxiliary nuisance cost-vector model. We extend the decision-focused plug-in term to accommodate a broad class of DFL surrogates (e.g., SPO+, Perturbation Gradient (PG), and Perturbed Fenchel–Young Loss (PFYL)). *Second*, we exploit a universal-minimizer property of the nuisance least-squares objective to analyze the nuisance update as standalone online convex optimization against a fixed comparator, independently of the policy iterates. We then convert the resulting regret into a bias bound on the plug-in gradient via a one-step policy descent inequality, yielding $\mathcal{O}(T^{-1/2})$ stationarity. The same argument extends to the surrogate variant. *Third*, numerical experiments on top- k selection, shortest path, combinatorial pricing, and a real-data energy-scheduling benchmark show lower cumulative regret than contextual-bandit baselines.

1.1 Literature review

Decision-focused and predict-then-optimize learning. Decision-focused learning trains predictive models through the downstream optimization problems that consume their outputs (Mandi et al., 2024). For linear objectives, Smart Predict-then-Optimize (SPO) and SPO+ give a task-aware alternative to prediction error (Elmachoub and Grigas, 2022). Later methods develop differentiable perturbation-based optimizers and directional-gradient estimators (Berthet et al., 2020; Gupta and Huang, 2024). Score function estimators extend DFL to cases where direct differentiation through the task loss or optimization layer is difficult (Silvestri et al., 2026), and distributional DFL methods model uncertainty in optimization parameters using generative predictors such as conditional normalizing flows and diffusion models (Wang et al., 2026; Zhao et al., 2026). Our proposed method inherits the use of distributional predictions and score function gradients, but the observation model differs: the learning signal is online, with policy-generated partial feedback rather than observed cost vectors. Sequential DFL methods include online predict-then-optimize (Liu and Grigas, 2022) and multi-stage

Predict+Optimize with sequential parameter revelation and interleaved decisions (Hu et al., 2024a); the closest theoretical analog is online DFL for linear optimization over polytopes (Capitaine et al., 2026). All three share our sequential viewpoint but assume full-information feedback rather than the partial feedback induced by the implemented decision.

Contextual optimization with partial feedback. The closest contextual optimization precursor is Hu et al. (2024b), who study offline contextual linear optimization under partial feedback (pure bandit and semi-bandit). Their work develops, from logged partial-feedback data, induced-ERM and surrogate approaches using least-squares nuisance estimation. Other work studies partial information from different angles. Ye et al. (2025) use distributional predictions for mixed-integer and nonlinear contextual stochastic optimization. Bennouna et al. (2025, 2026) study data informativeness for linear optimization, characterizing when partial observations contain enough information to identify an optimal decision. This paper studies the online counterpart. At each iteration, the current policy and optimization oracle choose a feasible decision. Feedback is observed only for that decision, from aggregate loss in the pure bandit case to selected component observations in semi-bandit variants. The same stream of partial feedback is used both to estimate the cost model and to update the policy.

Contextual bandits and policy optimization. Contextual bandits provide the standard framework for sequential learning from partial feedback (Li et al., 2010; Abbasi-Yadkori et al., 2011; Bubeck and Cesa-Bianchi, 2012). Work on large or structured action spaces includes contextual semi-bandits and oracle-based methods (Krishnamurthy et al., 2016; Zhu et al., 2022; Zierahn et al., 2023). Structured prediction with bandit feedback is also related: a learner outputs a structured object and observes only its task loss (Sokolov et al., 2016; Kreutzer et al., 2017). Our score function estimator follows the likelihood-ratio principle of REINFORCE and policy-gradient methods (Williams, 1992; Sutton et al., 2000; Konda and Tsitsiklis, 2000). Unlike standard contextual-bandit models that parameterize rewards over context-action pairs, we keep the linear-cost representation explicit, sampling a cost-vector prediction and solving a known optimization problem, while the auxiliary estimator learns conditional cost structure from partial observations.

Online convex optimization. Online convex optimization (OCO) and its bandit variants study sequential convex or linear losses with full-information or bandit feedback (Zinkevich, 2003; Flaxman et al., 2005; Dani et al., 2008; Abernethy et al., 2008; Ito et al., 2019), bounding regret against the best fixed decision in hindsight. Our setting is one step removed: we update parameters of a stochastic policy that produces a decision via the optimization oracle, and because the induced policy objective is nonsmooth and non-convex, our analysis targets first-order stationarity rather than convex regret.

2 Decision-focused on-policy learning with partial feedback

We consider a sequential contextual stochastic linear optimization setting. At each time $t = 1, 2, \dots$, the decision-maker observes a context $x_t \in \mathcal{X} \subseteq \mathbb{R}^{d_x}$ (context dimension d_x) and then makes a decision $w_t \in \mathcal{S}$, where $\mathcal{S} \subset \mathbb{R}^{d_w}$ is a compact feasible set. The context x_t is drawn from an unknown marginal distribution \mathcal{D}_x . Furthermore, the latent cost vector $c_t \sim p^*(\cdot | x_t)$ is never observed directly: once a decision is made, the learner sees only a partial-feedback vector $v_t \in \mathbb{R}^{d_v}$ (with feedback dimension d_v) whose form depends on the implemented decision; for instance, a selected route reveals the realized travel time of the chosen path, not the time on every edge. We denote the unknown joint distribution of $(x_t, c_t) \in \mathcal{X} \times \mathbb{R}^{d_w}$ by \mathcal{D} (assumed to be i.i.d. over time).

Assumption 1 (Feedback structure). *At each time $t = 1, 2, \dots$, given that $(x_t, c_t) \sim \mathcal{D}$, we have the following:*

1. *For every possible decision $w_t \in \mathcal{S}$, there exists a known observation matrix $H(w_t) \in \mathbb{R}^{d_v \times d_w}$ such that the observed feedback $v_t \in \mathbb{R}^{d_v}$ satisfies $v_t = H(w_t)c_t$.*
2. *For every possible decision $w_t \in \mathcal{S}$, there exists a known linkage vector $e(w_t) \in \mathbb{R}^{d_v}$ such that $H(w_t)^\top e(w_t) = w_t$; consequently, $y_t = c_t^\top w_t = e(w_t)^\top v_t$ is always recoverable.*

In words, $H(w_t)$ selects which linear measurements of the latent cost vector are revealed by decision w_t , and $e(w_t)$ is a known weight vector whose inner product with the observation always returns the realized scalar cost: $e(w_t)^\top v_t = c_t^\top w_t = y_t$, regardless of the feedback regime. For example,

pure bandit feedback ($H(w) = w^\top$, $e(w) = 1$) is the trivial case where v_t is already that scalar cost; Appendix A instantiates the full-information and semi-bandit cases.

In contextual linear optimization, a key assumption is that we can readily solve linear optimization problems over the compact decision set \mathcal{S} ; let $w^*(\hat{c}) \in \arg \min_{w \in \mathcal{S}} \hat{c}^\top w$ denote a particular linear optimization oracle for \mathcal{S} . We consider a class of distributional plug-in/predict-then-optimize policies, whereby $p_\theta(\cdot | x)$ denotes a parametric conditional model for cost vector predictions, parameterized by $\theta \in \mathbb{R}^{d_\theta}$. Any $\theta \in \mathbb{R}^{d_\theta}$ induces a policy $\pi_\theta : \mathcal{X} \rightarrow \Delta(\mathcal{S})$, where $\Delta(\mathcal{S})$ is the set of all distributions supported on \mathcal{S} , via the pushforward of $p_\theta(\cdot | x)$ by w^* , i.e., given observed context $x_t \in \mathcal{X}$ at time t , we first sample a predicted cost vector $\hat{c}_t \sim p_\theta(\cdot | x_t)$ and then make the decision $w_t = w^*(\hat{c}_t)$. Given $\theta \in \mathbb{R}^{d_\theta}$, let us also define the mean prediction function $\bar{\mu}_\theta(x) := \mathbb{E}_{\hat{c} \sim p_\theta(\cdot | x)} [\hat{c}]$ and the mean decision function $w_\theta^*(x) := \mathbb{E}_{\hat{c} \sim p_\theta(\cdot | x)} [w^*(\hat{c})]$. Furthermore, for a given parameter θ , let \mathcal{D}_θ denote the distribution over (x, c, w) induced by $(x, c) \sim \mathcal{D}$ and $w \sim \pi_\theta(\cdot | x)$. An important observation is that the conditional independence property $w \perp c | x$ holds for $(x, c, w) \sim \mathcal{D}_\theta$.

Let $f^*(x) := \mathbb{E}_{c \sim p^*(\cdot | x)} [c]$ denote the ground truth regression function. We define the expected cost of policy parameterized by $\theta \in \mathbb{R}^{d_\theta}$ by

$$V^{\text{cost}}(\theta) := \mathbb{E}_{(x, c, w) \sim \mathcal{D}_\theta} [c^\top w] = \mathbb{E}_{x \sim \mathcal{D}_x} [\mathbb{E}_{c \sim p^*(\cdot | x)} [c^\top w_\theta^*(x)]] = \mathbb{E}_{x \sim \mathcal{D}_x} [f^*(x)^\top w_\theta^*(x)],$$

where the latter equalities use $w \perp c | x$. It is well known and apparent from the above that, under full information, the decision maker would ideally make decision $w^*(f^*(x))$. Therefore, any policy such that $w_\theta^*(x) = w^*(f^*(x))$ almost surely over x is an optimal full information policy, for example a degenerate distribution with $\bar{\mu}_\theta(x) = f^*(x)$. Our primary reasons for focusing on a *distributional* plug-in class, instead of a point prediction class, are to ensure smoothness of $V^{\text{cost}}(\cdot)$ and to enable the score function and decision-focused gradient estimators that we develop below.

2.1 Score function gradient estimation

Our distributional plug-in policies correspond to the perturbed optimizer $w_\theta^*(\cdot)$ framework of Berthet et al. (2020); key regularity properties are discussed in Appendix B. Note that θ enters $V^{\text{cost}}(\theta)$ only through the sampling distribution $p_\theta(\cdot | x)$, not through the cost or the optimizer $w^*(\cdot)$. This key structural property enables score function based gradient estimation directly from bandit feedback, without differentiating through w^* , which aligns with our motivation for using a distributional/perturbed policy class.

Full details of the score function gradient estimator derivation are given in Appendix D; in short, given current parameters θ_t at time t , under well-behaved parametric distributions, differentiating under the expectation yields the one-sample score function gradient estimator

$$g_t^{\text{score}} := y_t \nabla_\theta \log p_{\theta_t}(\hat{c}_t | x_t), \quad \text{where} \quad \hat{c}_t \sim p_{\theta_t}(\cdot | x_t), w_t = w^*(\hat{c}_t), y_t = c_t^\top w_t, \quad (1)$$

which satisfies $\mathbb{E}[g_t^{\text{score}}] = \nabla_\theta V^{\text{cost}}(\theta_t)$. Note that g_t^{score} depends on the environment only through the scalar bandit feedback y_t , with no explicit reference to f^* . More generally, any terms preserving unbiasedness of the gradient estimator of $\nabla_\theta V^{\text{cost}}(\theta)$ may replace y_t in (1); for instance, subtracting a context-dependent baseline $b(x_t)$ from y_t preserves unbiasedness while typically reducing variance, an idea long exploited in the policy-gradient literature.

2.2 Decision-focused gradient estimation

The score function gradient estimator, while unbiased, is structure-agnostic: it treats y_t as a generic scalar cost and only weakly exploits the linear optimization structure. Decision-focused methods in the full-information setting instead exploit the direct dependence of $w_\theta^*(\cdot)$ on θ . Furthermore, particularly in the case of contextual linear optimization, the decomposition of V^{cost} above reveals that $V^{\text{cost}}(\theta)$ depends on the cost distribution *only* through its conditional mean $f^*(x) = \mathbb{E}[c | x]$. At the same time, the observed feedback v_t carries information about f^* that the score estimator never directly exploits. These observations suggest a complementary route: estimate f^* from accumulated feedback, plug the resulting nuisance estimate into $V^{\text{cost}}(\cdot)$, and apply standard full-information decision-focused machinery such as direct gradients and surrogate losses. This decision-focused, plug-in perspective trades the unbiasedness of (1) for exploitation of the downstream optimization problem and a potentially substantial reduction in variance.

Nuisance estimation via least-squares feedback fitting. We introduce an auxiliary cost-vector regression model $f_\phi : \mathcal{X} \rightarrow \mathbb{R}^{d_w}$ (the *nuisance* estimator, following Hu et al. (2024b)), parameterized by $\phi \in \Phi \subset \mathbb{R}^{d_\phi}$, which approximates the conditional cost mean $f^*(x) = \mathbb{E}[c \mid x]$ by minimizing the following least-squares objective based on the observed feedback $v = H(w)c$.

$$\min_{\phi \in \Phi} \mathcal{R}_\theta(f_\phi) = \mathbb{E}_{(x,c,w) \sim \mathcal{D}_\theta} [\|v - H(w)f_\phi(x)\|^2] \quad (2)$$

Remark 2.1 (Universal minimizer). *A key property of this objective is that f^* is a universal minimizer of \mathcal{R}_θ for every $\theta \in \mathbb{R}^{d_\theta}$. Consequently, the nuisance estimation target does not shift with the policy, which is central to our analysis. We assume realizability in parameter space: there exists $\phi^* \in \Phi$ such that $f_{\phi^*} = f^*$.*

The regret analysis of the nuisance model is obtained using standard online convex optimization results and universality of the minimizer. We defer the full analysis of the nuisance estimator to Appendix C.

Proposition 2.1 (Nuisance regret). *Suppose Φ is convex and compact with diameter D_Φ , the loss satisfies $G_{\mathcal{R}}$ -bounded gradients and $\nabla_\phi^2 \mathcal{R}_\theta(f_\phi) \succeq \lambda I$ for every θ . Under realizability ($f^* \in \mathcal{F}$), for any sequence $\{\theta_t\}_{t=1}^T$, the average excess nuisance loss satisfies*

$$\begin{aligned} \text{(i)} \quad & \frac{1}{T} \sum_{t=1}^T \mathbb{E}[\mathcal{R}_{\theta_t}(f_{\phi_t}) - \mathcal{R}_{\theta_t}(f^*)] \leq \frac{D_\Phi G_{\mathcal{R}}}{\sqrt{T}} \quad \text{with } \eta = D_\Phi / (G_{\mathcal{R}} \sqrt{T}); \\ \text{(ii)} \quad & \frac{1}{T} \sum_{t=1}^T \mathbb{E}[\mathcal{R}_{\theta_t}(f_{\phi_t}) - \mathcal{R}_{\theta_t}(f^*)] \leq \frac{G_{\mathcal{R}}^2 (1 + \log T)}{2\lambda T} \quad \text{with } \eta_t = 1/(\lambda t). \end{aligned}$$

The uniform strong-convexity condition $\nabla_\phi^2 \mathcal{R}_\theta(f_\phi) \succeq \lambda I$ for every θ is an identifiability/exploration assumption on the policy-induced feedback; under pure bandit feedback it requires the sampled actions to span the cost directions relevant to the nuisance class. This regret bound is the primary tool for controlling the bias of the plug-in gradient estimator introduced next. Given a nuisance estimate f_ϕ , we define the plug-in policy objective, which is an approximation of $V^{\text{cost}}(\theta)$, by

$$J(\phi, \theta) := \mathbb{E}_{x \sim \mathcal{D}_x} [f_\phi(x)^\top w_\theta^*(x)] = \mathbb{E}_{x \sim \mathcal{D}_x, \hat{c} \sim p_\theta(\cdot | x)} [f_\phi(x)^\top w^*(\hat{c})]. \quad (3)$$

Plug-in gradient estimator. Under standard regularity assumptions (Appendix B), differentiating the plug-in objective yields

$$\nabla_\theta J(\phi, \theta) = \mathbb{E}_{x \sim \mathcal{D}_x} \left[(\nabla_\theta w_\theta^*(x))^\top f_\phi(x) \right], \quad \nabla_\theta w_\theta^*(x) \in \mathbb{R}^{d_w \times d_\theta}. \quad (4)$$

Since θ enters $J(\phi, \theta)$ solely through the sampling distribution, computing $\nabla_\theta J(\phi, \theta)$ reduces to differentiating $w_\theta^*(x)$. For polyhedral \mathcal{S} and other cases, the mapping $\hat{c} \mapsto w^*(\hat{c})$ may be piecewise constant almost everywhere, so differentiating through it in the second expectation in (3) may yield uninformative gradients, making it difficult to obtain a one-sample stochastic gradient estimator of $\nabla_\theta J(\phi, \theta)$. One approach to overcome this challenge is to again rely on a score function representation:

$$g_t^{\text{plug-in}} = (w_t^\top f_{\phi_t}(x_t)) \nabla_\theta \log p_{\theta_t}(\hat{c}_t \mid x_t), \quad \text{where } \hat{c}_t \sim p_{\theta_t}(\cdot \mid x_t), w_t = w^*(\hat{c}_t). \quad (5)$$

Using the above estimator resembles a traditional actor-critic method; however, again it only weakly exploits the optimization structure.

Surrogate plug-in gradient estimator. To better exploit the linear optimization structure, we build on the extensive literature of decision-focused *surrogate* methods that have been developed in the full information setting. Namely, we replace $f_\phi(x)^\top w^*(\hat{c})$ in (3) by a differentiable proxy $h^{\text{sur}}(f_\phi(x), \hat{c})$ designed to provide informative gradients. Examples include the SPO+ loss (Elmachtoub and Grigas, 2022), the Fenchel-Young loss (Berthet et al., 2020), and the Perturbation Gradient loss (Gupta and Huang, 2024), among others. For any choice of surrogate function $h^{\text{sur}}(f_\phi(x), \hat{c})$, we define the surrogate plug-in objective

$$J^{\text{sur}}(\phi, \theta) := \mathbb{E}_{x \sim \mathcal{D}_x, \hat{c} \sim p_\theta(\cdot | x)} [h^{\text{sur}}(f_\phi(x), \hat{c})]. \quad (6)$$

Unlike the plug-in objective $J(\phi, \theta)$, which requires differentiating through $w_\theta^*(x)$, we instead differentiate through the surrogate $h^{\text{sur}}(f_\phi(x), \hat{c})$, which is engineered to have informative gradients almost everywhere. Combined with a reparameterization $\hat{c} = \mu_\theta(x, \varepsilon)$ with $\varepsilon \sim \nu$ independent of θ (Assumption 4 in Appendix B), this yields the surrogate gradient estimator $g_t^{\text{sur}} =$

$(\nabla_{\theta} \mu_{\theta_t}(x_t, \varepsilon_t))^{\top} \nabla_{\hat{c}} h^{\text{sur}}(f_{\phi_t}(x_t), \hat{c}_t)$. Conditioned on (ϕ_t, θ_t) , g_t^{sur} is unbiased for $\nabla_{\theta} J^{\text{sur}}(\phi_t, \theta_t)$; bias relative to V^{cost} comes from the nuisance estimate and the surrogate choice. The full surrogate framework is in Appendix E.

2.3 Decision-focused hybrid policy gradient algorithm

The score function gradient estimator (1) and the plug-in objective (3) (or its surrogate function variant (6)) provide two complementary gradient signals for θ . Our algorithm exploits both: at each iteration, it updates the nuisance parameter ϕ by least-squares SGD step on (2), and the parameter θ by an SGD step combining the two signals. This complementarity motivates combining them through a convex mixture. For a mixing parameter $\alpha \in [0, 1]$, we define the hybrid gradient estimator

$$g_t^{\alpha} = \alpha g_t^{\text{score}} + (1 - \alpha) g_t^{\text{plug-in}} \quad (7)$$

The surrogate variant of the hybrid estimator is obtained by substituting g_t^{sur} for $g_t^{\text{plug-in}}$, yielding $g_t^{\alpha, \text{sur}} := \alpha g_t^{\text{score}} + (1 - \alpha) g_t^{\text{sur}}$. At $\alpha = 1$ the estimator reduces to the unbiased score function gradient, while at $\alpha = 0$ it relies entirely on the plug-in gradient.

Algorithm 1 instantiates this construction as an online procedure covering both the plug-in and surrogate variants.

Algorithm 1: Decision-focused hybrid policy gradient (DFHPG)

Input: Initial parameters $\phi_1 \in \Phi$, $\theta_1 \in \mathbb{R}^{d_{\theta}}$; mixing parameter $\alpha \in [0, 1]$; step sizes $\eta_t, \beta > 0$
for $t = 1, 2, \dots, T$ **do**

 Observe context x_t ;

 Sample $\hat{c}_t \sim p_{\theta_t}(\cdot | x_t)$ and execute $w_t \in \arg \min_{w \in \mathcal{S}} \hat{c}_t^{\top} w$;

 Observe feedback v_t and set $y_t = e(w_t)^{\top} v_t$;

$\phi_{t+1} = \Pi_{\Phi}(\phi_t - \eta_t \nabla_{\phi} \ell_t(\phi_t))$, $\ell_t(\phi) = \|v_t - H(w_t) f_{\phi}(x_t)\|^2$ // Nuisance update

$\theta_{t+1} = \theta_t - \beta \tilde{g}_t$, where $\tilde{g}_t = g_t^{\alpha}$ for the plug-in variant and $\tilde{g}_t = g_t^{\alpha, \text{sur}}$ for the surrogate variant // Hybrid policy update

2.4 Convergence results

We formalize the convergence guarantees of Algorithm 1. Since the objective is non-convex in θ , we target standard non-convex stationarity criteria. The analysis hinges on a key structural property: the hybrid update is conditionally biased only through the nuisance error, which is in turn controlled by the regret of the nuisance update (Proposition 2.1). Under regularity assumptions on the parametric family p_{θ} , the distributional smoothing $w_{\theta}^*(x)$ is differentiable and Lipschitz even though the underlying map $\hat{c} \mapsto w^*(\hat{c})$ is piecewise constant, yielding L_{θ}^J -smoothness of the plug-in objective $J(\phi, \theta)$ in θ with gradient norm bounded by G^J . The full regularity analysis is deferred to Appendix D.

Theorem 2.2 (Non-convex stationarity, plug-in variant). *Let $V^* := \inf_{\theta} V^{\text{cost}}(\theta) > -\infty$. With step size $\beta = 1/(L_{\theta}^J \sqrt{T})$, Algorithm 1 satisfies*

(i) With $\eta_t = D_{\Phi}/(G_{\mathcal{R}} \sqrt{T})$:

$$\frac{1}{T} \sum_{t=1}^T \mathbb{E}[\|\nabla_{\theta} V^{\text{cost}}(\theta_t)\|^2] \leq \frac{2L_{\theta}^J \Delta_1 + (G^J)^2 + \sigma_{\alpha}^2}{\sqrt{T}} + \mathcal{O}\left(\frac{(1 - \alpha)^2 D_{\Phi} G_{\mathcal{R}}}{\lambda \sqrt{T}}\right), \quad (8)$$

(ii) With $\eta_t = 1/(\lambda t)$:

$$\frac{1}{T} \sum_{t=1}^T \mathbb{E}[\|\nabla_{\theta} V^{\text{cost}}(\theta_t)\|^2] \leq \frac{2L_{\theta}^J \Delta_1 + (G^J)^2 + \sigma_{\alpha}^2}{\sqrt{T}} + \mathcal{O}\left(\frac{(1 - \alpha)^2 (1 + \log T)}{\lambda^2 T}\right), \quad (9)$$

where $\Delta_1 := V^{\text{cost}}(\theta_1) - V^*$, and the variance $\sigma_{\alpha}^2 := (\alpha \sigma_{\text{score}} + (1 - \alpha) \sigma_{\text{plug-in}})^2$.

The bound above decomposes cleanly into an optimization term, depending on the smoothness and variance properties of the plug-in objective, and a bias term, controlled entirely by the nuisance estimator convergence. The optimization term is $\mathcal{O}(T^{-1/2})$ in both cases, matching the standard non-convex SGD rate (Ghadimi and Lan, 2013). The bias term vanishes whenever $f_{\phi_t} = f^*$, since $J(\phi, \theta)$ and $V^{\text{cost}}(\theta)$ differ only through the substitution of f_ϕ for f^* . The two step-size schedules correspond to the two cases of Proposition 2.1: the constant schedule yields a bias of the same $\mathcal{O}(T^{-1/2})$ order as the optimization term, while the adaptive schedule sharpens it to $\mathcal{O}(\log T/T)$, leaving the optimization term as the sole dominant contribution.

Supporting lemmas and proofs are deferred to Appendices C, D and E.

The variance σ_α^2 interpolates continuously between two extremes. At $\alpha = 1$ one recovers the unbiased score function gradient (Sutton and Barto, 2018). At $\alpha = 0$ one relies entirely on the plug-in gradient, which enjoys lower variance once f_{ϕ_t} is well-trained, at the cost of a nuisance-driven bias. The optimal α shifts toward zero as the nuisance estimation improves, suggesting that adaptive schedules $\alpha_t \rightarrow 0$ may improve empirical performance.

We now turn to the surrogate variant. Define $V^\alpha(\theta) := \alpha V^{\text{cost}}(\theta) + (1 - \alpha) J^{\text{sur}}(\phi^*, \theta)$. The smoothness of V^α follows from that of its two components: $V^{\text{cost}}(\theta) = J(\phi^*, \theta)$ inherits L_θ^J -smoothness from the plug-in analysis above, while $J^{\text{sur}}(\phi^*, \cdot)$ is smooth by virtue of the regularity of both the reparameterization map μ_θ and the surrogate gradient $\nabla_{\hat{c}} h^{\text{sur}}$. As a convex combination of smooth functions, V^α is therefore L_θ^α -smooth with gradient norm bounded by \tilde{G}_α ; the full derivation is in Appendix E. We state the result under the dynamic schedule $\eta_t = 1/(\lambda t)$; an analogous bound to Theorem 2.2(i) holds for the constant step size for our surrogate model.

Theorem 2.3 (Non-convex stationarity, surrogate variant). *Let $V^{\alpha,*} := \inf_\theta V^\alpha(\theta)$. Running Algorithm 1 with $\beta = 1/(L_\theta^\alpha \sqrt{T})$ and $\eta_t = 1/(\lambda t)$ yields*

$$\frac{1}{T} \sum_{t=1}^T \mathbb{E}[\|\nabla V^\alpha(\theta_t)\|^2] \leq \frac{2L_\theta^\alpha \Delta_1^\alpha + \tilde{G}_\alpha^2 + \tilde{\sigma}_\alpha^2}{\sqrt{T}} + \mathcal{O}\left((1 - \alpha)^2 \frac{1 + \log T}{\lambda^2 T}\right). \quad (10)$$

with $\Delta_1^\alpha = V^\alpha(\theta_1) - V^{\alpha,*}$, $\tilde{\sigma}_\alpha^2 := (\alpha \sigma_{\text{score}} + (1 - \alpha) \sigma_{\text{sur}})^2$.

Theorem 2.3 guarantees stationarity for V^α , not directly for V^{cost} ; the surrogate-to-task gap depends on the chosen DFL surrogate and is not formally quantified here. The bound mirrors the structure of Theorem 2.2, with a dominant $\mathcal{O}(T^{-1/2})$ optimization term and a bias decaying at $\mathcal{O}(\log T/T)$ under the adaptive nuisance schedule. The bias is controlled by the Lipschitz constant of $\nabla_{\hat{c}} h^{\text{sur}}$ with respect to its cost argument, measuring how sensitively the surrogate gradient responds to shifts in the nuisance estimate away from f^* ; explicit constants are provided in Appendix E. The surrogate variant is preferred in practice because it provides more informative gradient signals than the plug-in estimator, which must rely on the score function representation to circumvent the piecewise-constant nature of $\hat{c} \mapsto w^*(\hat{c})$.

3 Numerical experiments

3.1 Benchmark problems

The experiments use four online contextual optimization benchmarks with bandit feedback: three synthetic linear-objective tasks (top- k selection, shortest path, and combinatorial pricing) and a real-data energy-scheduling instance. At each iteration t , a context x_t is observed, a feasible decision is selected by solving an optimization problem with predicted parameters, and only the realized scalar objective value of the selected decision is observed. For linear-objective benchmarks, this feedback takes the form $v_t = c_t^\top w_t$, where the latent cost vector $c_t \sim p^*(\cdot | x_t)$ is not revealed. Benchmark data details (synthetic data generation and the energy-scheduling data source and chronological split) are collected in Appendix F; semi-bandit and full-information variants of the feedback model are reported in Appendix K.7.

Top- k selection. This benchmark models the selection of exactly k items from the candidate set $\mathcal{I}_{\text{top}} = \{1, \dots, d\}$. The binary decision variable w_i indicates whether item i is selected. Given

predicted item costs \hat{c}_t , the top- k oracle solves

$$\min_{w \in \{0,1\}^d} \hat{c}_t^\top w \quad \text{s.t.} \quad \mathbf{1}^\top w = k.$$

Shortest path. This benchmark uses a fixed directed acyclic grid $\mathcal{G} = (\mathcal{V}, \mathcal{E})$ with right/down edges, where $|\mathcal{V}| = 25$ and $|\mathcal{E}| = q = 40$. The binary decision variable w_e indicates whether edge e is on the selected path. Let A denote the node-arc incidence matrix and $b_{sd} \in \mathbb{R}^{|\mathcal{V}|}$ the source-destination balance vector (+1 at the source, -1 at the destination, 0 elsewhere). Given predicted edge costs \hat{c}_t , the shortest-path oracle solves

$$\min_{w \in \{0,1\}^q} \hat{c}_t^\top w \quad \text{s.t.} \quad Aw = b_{sd}.$$

Combinatorial pricing. This benchmark assigns one of K_{price} discrete price levels to each of n products. Let $w_{i\ell}$ indicate whether product i is assigned price level ℓ , let $L_{\text{promo}} \leq K_{\text{price}}$ be the number of lowest price tiers counted as promotional, and let B_{promo} be the promotion budget. Given predicted product-price costs \hat{c}_t , the induced decision solves

$$\min_{w \in \{0,1\}^{nK_{\text{price}}}} \hat{c}_t^\top w \quad \text{s.t.} \quad \sum_{\ell=1}^{K_{\text{price}}} w_{i\ell} = 1 \quad \forall i, \quad \sum_{i=1}^n \sum_{\ell=1}^{L_{\text{promo}}} w_{i\ell} \leq B_{\text{promo}}.$$

Conditional on x_t , latent demand is sampled for every product-price pair; the action determines which entries are monetized, and the benchmark is written as cost minimization with cost equal to negative realized revenue.

Energy scheduling. This benchmark schedules tasks on machines under day-ahead electricity prices, following Mandi et al. (2024) with empirical SEMO data. Each iteration t corresponds to one day. Each task j has duration d_j slots, and each resource u has machine- m capacity $\bar{\rho}_{mu}$ and per-task usage ρ_{ju} . The binary decision $w_{jms} \in \{0,1\}$ indicates that task j starts on machine m at slot s , with $w \in \{0,1\}^{d_w}$ indexing feasible (task, machine, start-slot) triples. Aggregating the day’s per-slot prices over each task’s run window yields an iteration- t cost vector $c_t \in \mathbb{R}^{d_w}$ that depends linearly on the price profile. Given a predicted cost \hat{c}_t , the scheduling oracle solves

$$\min_{w \in \{0,1\}^{d_w}} \hat{c}_t^\top w \quad \text{s.t.} \quad \sum_{m,s} w_{jms} = 1 \quad \forall j, \quad \sum_j \rho_{ju} \sum_{s:s \leq s' < s+d_j} w_{jms} \leq \bar{\rho}_{mu} \quad \forall (m, u, s').$$

3.2 Experimental setup

The proposed method is reported as DFHPG. It uses the hybrid gradient update in Algorithm 1, with the fixed mixing weight α replaced by a time-varying α_t decaying from α_{\max} to α_{\min} . The score function gradient subtracts a variance-reduction baseline b_t . Two ablations isolate the two gradient components: DFHPG-1 uses only the score function update, DFHPG-0 only the plug-in update. Theorems 2.2 and 2.3 cover the fixed- α plug-in and surrogate variants. The experiments include three heuristic modifications outside the theory: the time-varying α_t schedule (Appendix J), the variance-reduction baseline subtracted from the score function term (Appendix I), and separate L_2 normalization of the score and plug-in components before mixing (Appendix L.2).

We compare against three contextual-bandit-style baselines that share DFHPG’s context, feedback, and linear optimization oracle, isolating the effect of the learning update from the action-selection rule. GREEDYCB uses greedy exploitation with a point cost predictor; ϵ -GREEDYCB adds random exploration; TSCB samples a cost vector from the learned conditional cost distribution and solves the linear optimization at that sample, matching Thompson sampling’s action-level randomization without an explicit Bayesian posterior. LinUCB and OFUL require a stronger oracle than linear minimization and fall outside this matched setup. Pseudocode is in Appendix G.

The default distributional cost-vector prediction model is the Gaussian linear model; the Gaussian neural-network (NN), conditional normalizing-flow (CNF), and denoising diffusion probabilistic model (DDPM) variants are also supported and reported as alternatives in Section 3.3 and Appendix K.2. The Gaussian variants set $p_\theta(\cdot | x) = \mathcal{N}(\bar{\mu}_\theta(x), \sigma_G^2 I_{d_w})$, where $\bar{\mu}_\theta$ is the mean

prediction function parameterized either as a linear map (Gaussian linear) or as a two-layer neural network with 128 hidden units (Gaussian NN), and $\sigma_G > 0$ is a fixed exploration scale. The CNF variant uses a two-layer conditional RealNVP flow (Dinh et al., 2017) with 128-dimensional coupling networks; the DDPM variant uses a conditional denoiser (Ho et al., 2020) with a 128-dimensional hidden layer. Update rules for the generative variants are in Appendix H. The main metric reported is cumulative regret, $\text{Regret}_T = \sum_{t=1}^T (c_t^\top w_t - \min_{w \in \mathcal{S}} c_t^\top w)$, where $w_t \in \mathcal{S}$ is the decision implemented at iteration t . Convergence figures plot the ergodic average regret per iteration, Regret_t/t .

3.3 Results

Table 1 reports final cumulative regret across the four benchmarks under both feedback regimes. Under pure bandit feedback, DFHPG achieves the lowest regret on top- k selection, shortest path, and pricing, with DFHPG-0 second-best in each; on energy, both DFHPG and DFHPG-0 beat the contextual-bandit baselines by roughly 1.7–1.9 \times , and DFHPG-0 slightly outperforms the hybrid update (within one standard error), consistent with the higher regret of DFHPG-1 and indicating that the score function signal is too noisy on this low-signal real-data instance. Semi-bandit feedback drops cumulative regret by roughly 50–75% on the synthetic benchmarks and $\sim 35\%$ on energy, with DFHPG-0 winning every column (including the semi-bandit-adapted CB baselines, Appendix K.7): the coordinate-level signal flows directly into the nuisance fit and sharpens the plug-in gradient, leaving little to gain from the score function term, which is therefore most useful in the pure-bandit regime.

Table 1: Final cumulative regret across benchmarks. The first three columns are synthetic degree-8 Gaussian linear cost-model experiments at horizon $T = 2,000$; the fourth is the real-data energy-scheduling benchmark. The top block reports pure bandit feedback, the bottom block semi-bandit feedback. Entries report mean \pm standard error over 30 replications; lower is better. Within each block, the best result is bolded and the second-best is underlined.

Method	Top- k (deg. 8)	Shortest path (deg. 8)	Pricing (deg. 8)	Energy
<i>Pure bandit feedback</i>				
GREEDYCB	$6.94 \times 10^5 \pm 3.38 \times 10^4$	$1.98 \times 10^6 \pm 4.40 \times 10^4$	$7.41 \times 10^4 \pm 1.23 \times 10^4$	$6.43 \times 10^7 \pm 1.95 \times 10^5$
ϵ -GREEDYCB	$7.17 \times 10^5 \pm 3.98 \times 10^4$	$2.06 \times 10^6 \pm 4.12 \times 10^4$	$7.89 \times 10^4 \pm 1.10 \times 10^4$	$6.58 \times 10^7 \pm 3.01 \times 10^5$
TSCB	$6.93 \times 10^5 \pm 3.87 \times 10^4$	$2.00 \times 10^6 \pm 4.37 \times 10^4$	$7.33 \times 10^4 \pm 1.23 \times 10^4$	$6.43 \times 10^7 \pm 1.94 \times 10^5$
DFHPG-1	$4.00 \times 10^5 \pm 4.49 \times 10^4$	$1.81 \times 10^6 \pm 6.08 \times 10^4$	$6.46 \times 10^4 \pm 1.16 \times 10^4$	$1.60 \times 10^8 \pm 1.86 \times 10^7$
DFHPG	$1.68 \times 10^5 \pm 1.47 \times 10^4$	$1.50 \times 10^6 \pm 5.04 \times 10^4$	$2.98 \times 10^4 \pm 7.59 \times 10^3$	$3.85 \times 10^7 \pm 8.79 \times 10^6$
DFHPG-0	<u>$1.99 \times 10^5 \pm 2.38 \times 10^4$</u>	<u>$1.58 \times 10^6 \pm 5.15 \times 10^4$</u>	<u>$3.35 \times 10^4 \pm 8.09 \times 10^3$</u>	$3.50 \times 10^7 \pm 8.12 \times 10^6$
<i>Semi-bandit feedback</i>				
DFHPG	$7.10 \times 10^4 \pm 8.52 \times 10^3$	$6.83 \times 10^5 \pm 3.11 \times 10^4$	$7.54 \times 10^3 \pm 5.86 \times 10^2$	$2.35 \times 10^7 \pm 4.21 \times 10^5$
DFHPG-0	$6.65 \times 10^4 \pm 5.30 \times 10^3$	$5.31 \times 10^5 \pm 2.28 \times 10^4$	$7.30 \times 10^3 \pm 6.46 \times 10^2$	$2.33 \times 10^7 \pm 3.78 \times 10^5$

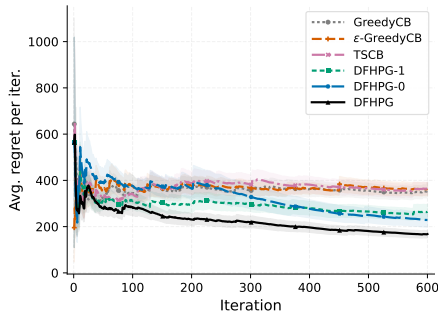


Figure 1: Zoomed convergence plot for top- k selection (first 600 iterations). Each curve reports average regret per iteration, with shaded ± 1 standard-error bands across replications.

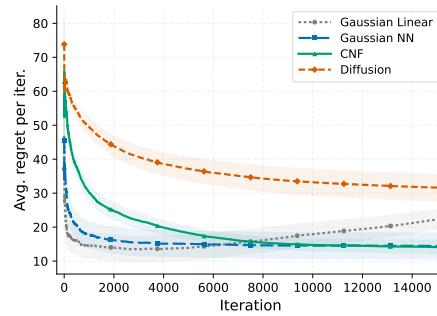


Figure 2: Comparison of distributional cost models on pricing at $T = 15,000$. Each curve reports average regret per iteration, with shaded ± 1 standard-error bands across replications.

Figure 1 traces top- k dynamics over the first 600 iterations and shows that the score function and plug-in components are complementary in time. For the first ~ 300 iterations DFHPG-1 sits below DFHPG-0: the score function gradient is unbiased and immediately usable, while the plug-in gradient relies on a nuisance that has not accumulated enough data. The order reverses past ~ 300 iterations, when the nuisance stabilizes and the lower-variance plug-in signal pulls DFHPG-0 below DFHPG-1; through its time-varying weighting, hybrid DFHPG absorbs both advantages and ends below the contextual-bandit baselines. Convergence plots for the other three benchmarks are in Appendix K.1.

Figure 2 explores distributional cost models on pricing at the extended horizon $T = 15,000$, revealing a data-vs-expressiveness trade-off. Early in training, when on-policy data is scarce, the simpler Gaussian linear model leads, quickly capturing the dominant linear cost structure with fewer parameters. As data accumulates, the more expressive CNF parameterization catches up and reaches lower final regret. Among the generative variants, CNF outperforms diffusion, possibly due to the tractable log-density of normalizing flows versus the evidence lower bound (ELBO) proxy used for diffusion. The same comparison on the other benchmarks, together with sensitivity studies (problem difficulty, mixing weight, surrogate loss, feedback mode), is in Appendix K.

4 Conclusion

This paper studies online contextual linear optimization under partial feedback and proposes a decision-focused hybrid policy gradient (DFHPG) method that combines an unbiased score function update with a plug-in update leveraging downstream optimization structure through a nuisance estimate of the latent cost vector. The analysis establishes convergence to first-order stationarity for the coupled policy and nuisance updates. On three synthetic benchmarks and a real-data energy-scheduling instance, DFHPG (strongest on synthetic) and the plug-in-only DFHPG-0 (marginally better on energy) both reduce final cumulative regret relative to contextual-bandit baselines and the score-only ablation; on energy, the score function signal is too noisy to add information beyond the plug-in component. The distributional algorithm extends naturally to nonlinear objectives, while the theory assumes linear objectives and exact oracle solves; extending it is left for future work.

Acknowledgments

This research was partly supported by the NSF AI Institute for Advances in Optimization (Award 2112533). The authors sincerely thank Amira Hijazi for discussions that helped scope this project.

References

- Abbasi-Yadkori, Y., Pál, D., and Szepesvári, C. (2011). Improved algorithms for linear stochastic bandits. *Advances in neural information processing systems*, 24.
- Abernethy, J., Hazan, E., and Rakhlin, A. (2008). Competing in the dark: An efficient algorithm for bandit linear optimization. In *Proceedings of the 21st Annual Conference on Learning Theory*, pages 263–273.
- Bennouna, O., Bennouna, A., Amin, S., and Ozdaglar, A. (2025). What data enables optimal decisions? an exact characterization for linear optimization.
- Bennouna, O., Bennouna, A., Amin, S., and Ozdaglar, A. (2026). Data informativeness in linear optimization under uncertainty.
- Berthet, Q., Blondel, M., Teboul, O., Cuturi, M., Vert, J.-P., and Bach, F. (2020). Learning with differentiable perturbed optimizers. In *Advances in Neural Information Processing Systems*, volume 33, pages 9508–9519.
- Bubeck, S. and Cesa-Bianchi, N. (2012). Regret analysis of stochastic and nonstochastic multi-armed bandit problems. *Foundations and Trends in Machine Learning*, 5(1):1–122.
- Capitaine, A., Haddouche, M., Moulines, E., Jordan, M. I., Boursier, E., and Durmus, A. O. (2026). Online decision-focused learning. In *International Conference on Learning Representations*.

- Dani, V., Hayes, T. P., and Kakade, S. M. (2008). Stochastic linear optimization under bandit feedback. In *Proceedings of the 21st Annual Conference on Learning Theory*, pages 355–366.
- Dinh, L., Sohl-Dickstein, J., and Bengio, S. (2017). Density estimation using real nvp. In *International Conference on Learning Representations*.
- Elmachtoub, A. N. and Grigas, P. (2022). Smart “predict, then optimize”. *Management Science*, 68(1):9–26.
- Flaxman, A. D., Kalai, A. T., and McMahan, H. B. (2005). Online convex optimization in the bandit setting: gradient descent without a gradient. In *Proceedings of the Sixteenth Annual ACM-SIAM Symposium on Discrete Algorithms, SODA '05*, pages 385–394, USA. Society for Industrial and Applied Mathematics.
- Ghadimi, S. and Lan, G. (2013). Stochastic first-and zeroth-order methods for nonconvex stochastic programming. *SIAM journal on optimization*, 23(4):2341–2368.
- Gupta, V. and Huang, M. (2024). Decision-focused learning with directional gradients. *Advances in Neural Information Processing Systems*, 37:79194–79220.
- Ho, J., Jain, A., and Abbeel, P. (2020). Denoising diffusion probabilistic models. *Advances in Neural Information Processing Systems*, 33:6840–6851.
- Hu, X., Lee, J. C. H., Lee, J. H. M., and Stuckey, P. J. (2024a). Multi-stage predict+optimize for (mixed integer) linear programs. *Advances in Neural Information Processing Systems*, 37:64794–64827.
- Hu, Y., Kallus, N., Mao, X., and Wu, Y. (2024b). Contextual linear optimization with bandit feedback. *Advances in Neural Information Processing Systems*, 37:26976–27004.
- Hu, Y., Kallus, N., Mao, X., and Wu, Y. (2025). Contextual linear optimization under partial feedback. *arXiv preprint arXiv:2405.16564*.
- Ito, S., Hatano, D., Sumita, H., Takemura, K., Fukunaga, T., Kakimura, N., and Kawarabayashi, K.-I. (2019). Oracle-efficient algorithms for online linear optimization with bandit feedback. In *Advances in Neural Information Processing Systems*, volume 32.
- Konda, V. R. and Tsitsiklis, J. N. (2000). Actor-critic algorithms. In *Advances in Neural Information Processing Systems*.
- Kreutzer, J., Sokolov, A., and Riezler, S. (2017). Bandit structured prediction for neural sequence-to-sequence learning. In *Proceedings of the 55th Annual Meeting of the Association for Computational Linguistics*, pages 1503–1513.
- Krishnamurthy, A., Agarwal, A., and Dudik, M. (2016). Contextual semibandits via supervised learning oracles. In *Advances in Neural Information Processing Systems*.
- Li, L., Chu, W., Langford, J., and Schapire, R. E. (2010). A contextual-bandit approach to personalized news article recommendation. In *Proceedings of the 19th international conference on World wide web*, pages 661–670.
- Liu, H. and Grigas, P. (2022). Online contextual decision-making with a smart predict-then-optimize method.
- Mandi, J., Bucarey, V., Tchomba, M. M. K., and Guns, T. (2022). Decision-focused learning: Through the lens of learning to rank. In *Proceedings of the International Conference on Machine Learning (ICML)*.
- Mandi, J., Kotary, J., Berden, S., Mulamba, M., Bucarey, V., Guns, T., and Fioretto, F. (2024). Decision-focused learning: Foundations, state of the art, benchmark and future opportunities. *Journal of Artificial Intelligence Research*, 80:1623–1701.
- Minervini, P., Franceschi, L., and Niepert, M. (2023). Adaptive perturbation-based gradient estimation for discrete latent variable models. In *Proceedings of the AAAI Conference on Artificial Intelligence*.

- Mulamba, M., Mandi, J., Diligenti, M., Lombardi, M., Bucarey, V., and Guns, T. (2021). Contrastive losses and solution caching for predict-and-optimize. In *Proceedings of the International Joint Conference on Artificial Intelligence (IJCAI)*.
- Niepert, M., Minervini, P., and Franceschi, L. (2021). Implicit MLE: Backpropagating through discrete exponential family distributions. In *Advances in Neural Information Processing Systems (NeurIPS)*.
- Orabona, F. (2019). A modern introduction to online learning.
- Powell, W. B. (2022). Designing lookahead policies for sequential decision problems in transportation and logistics. *IEEE Open Journal of Intelligent Transportation Systems*, 3:313–327.
- Sadana, U., Chenreddy, A., Delage, E., Forel, A., Frejinger, E., and Vidal, T. (2025). A survey of contextual optimization methods for decision-making under uncertainty. *European Journal of Operational Research*, 320(2):271–289.
- Sahoo, S. S., Paulus, A., Vlastelica, M., Musil, V., Kuleshov, V., and Martius, G. (2023). Backpropagation through combinatorial algorithms: Identity with projection works. In *International Conference on Learning Representations (ICLR)*.
- Silvestri, M., Berden, S., Signorelli, G., Mahmutoğulları, A. İ., Mandi, J., Amos, B., Guns, T., and Lombardi, M. (2026). Score function gradient estimation to widen the applicability of decision-focused learning. *Journal of Artificial Intelligence Research*, 85:1–34.
- Sokolov, A., Kreutzer, J., Riezler, S., and Lo, C. (2016). Stochastic structured prediction under bandit feedback. In *Advances in Neural Information Processing Systems*.
- Sutton, R. S. and Barto, A. G. (2018). *Reinforcement Learning: An Introduction*. MIT Press, 2 edition.
- Sutton, R. S., McAllester, D., Singh, S., and Mansour, Y. (2000). Policy gradient methods for reinforcement learning with function approximation. In *Advances in Neural Information Processing Systems*.
- Tang, B. and Khalil, E. B. (2024). PyEPO: A PyTorch-based end-to-end predict-then-optimize library for linear and integer programming. *Mathematical Programming Computation*, 16:297–335.
- Van Hentenryck, P. and Bent, R. (2006). *Online stochastic combinatorial optimization*. The MIT Press.
- Vlastelica, M., Paulus, A., Musil, V., Martius, G., and Rolínek, M. (2020). Differentiation of blackbox combinatorial solvers. In *International Conference on Learning Representations (ICLR)*.
- Wang, P. Z., Chen, S., Liang, J., Fioretto, F., and Zhu, S. (2026). Gen-DFL: Decision-focused generative learning for robust decision making. In *International Conference on Learning Representations*.
- Williams, R. J. (1992). Simple statistical gradient-following algorithms for connectionist reinforcement learning. *Machine Learning*, 8:229–256.
- Ye, T., Cheng, S., Hijazi, A., and Van Hentenryck, P. (2025). Contextual stochastic optimization for omnichannel multicourier order fulfillment under delivery time uncertainty. *Manufacturing & Service Operations Management*.
- Zhao, Z., Yeh, C., Kong, L., and Wang, K. (2026). Diffusion-DFL: Decision-focused diffusion models for stochastic optimization. In *International Conference on Learning Representations*.
- Zhu, Y., Foster, D. J., Langford, J., and Mineiro, P. (2022). Contextual bandits with large action spaces: Made practical. In *Proceedings of the 39th International Conference on Machine Learning*, volume 162 of *Proceedings of Machine Learning Research*, pages 27428–27453.
- Zierahn, L., van der Hoeven, D., Cesa-Bianchi, N., and Neu, G. (2023). Nonstochastic contextual combinatorial bandits. In *Proceedings of The 26th International Conference on Artificial Intelligence and Statistics*, volume 206 of *Proceedings of Machine Learning Research*, pages 8771–8813.

Zinkevich, M. (2003). Online convex programming and generalized infinitesimal gradient ascent. In *Proceedings of the 20th international conference on machine learning (icml-03)*, pages 928–936.

A Partial feedback structure examples

The feedback structure in Assumption 1 is flexible enough to capture several practically important settings. We highlight the three main instances considered in this paper.

- **Full feedback.** Set $H(w) = I$ and $e(w) = w$. The feedback coincides with the cost vector, $v = c$, and the linkage identity $c^\top w = e(w)^\top v$ holds trivially.
- **Bandit feedback.** Set $H(w) = w^\top$ and $e(w) = 1$. Then $v = c^\top w$ is the scalar realized cost, and the linkage identity reduces to $c^\top w = e(w)^\top v$, which holds trivially.
- **Semi-bandit / combinatorial feedback.** Let $\mathcal{S} \subseteq \{0, 1\}^d$. Set $H(w) = \text{diag}(w)$ and $e(w) = \mathbf{1}$. Then the feedback $v = \text{diag}(w)c$ records the cost of each selected coordinate. The linkage condition holds since $H(w)^\top e(w) = \text{diag}(w)\mathbf{1} = w$, and the identity $c^\top w = e(w)^\top v$ follows immediately.

B Regularity of the perturbed optimizer and score function representation

We consider the perturbed optimizers $w_\theta^*(x) := \mathbb{E}_{\hat{c} \sim p_\theta(\cdot | x)}[w^*(\hat{c})]$. The smoothing induced by p_θ makes $w_\theta^*(x)$ differentiable in θ even though the underlying optimizer $\hat{c} \mapsto w^*(\hat{c})$ is piecewise constant. The following assumptions and supporting results formalize this differentiability and the resulting regularity of the policy value V^{cost} .

Assumption 2 (Bounded feasible set and costs). \mathcal{S} is compact with $B_S := \sup_{w \in \mathcal{S}} \|w\| < \infty$, and there exists $B_c > 0$ such that $\|c_t\| \leq B_c$ almost surely.

Assumption 3 (Smooth parametric family). The parametric family $p_\theta(\cdot | x)$ is twice continuously differentiable in θ for all $x \in \mathcal{X}$, and there exist constants $M, M_\nabla < \infty$ such that for all $\theta, \theta' \in \mathbb{R}^{d_\theta}$ and $x \in \mathcal{X}$,

$$\int \|\nabla_\theta p_\theta(\hat{c} | x)\| d\hat{c} \leq M \quad (11)$$

$$\int \|\nabla_\theta p_\theta(\hat{c} | x) - \nabla_{\theta'} p_{\theta'}(\hat{c} | x)\| d\hat{c} \leq M_\nabla \|\theta - \theta'\| \quad (12)$$

Conditions (11)–(12) bound the parametric family in L^1 on the gradient and its variation, and are satisfied by all common smooth parameterizations, e.g., Gaussian families with smoothly parameterized mean and covariance, or exponential families with bounded sufficient statistics. They ensure that $\theta \mapsto \nabla_\theta w_\theta^*(x)$ is itself Lipschitz, which is needed to establish L_θ -smoothness of V^{cost} in Lemma D.1(ii).

Assumption 4 (Reparameterization). Under $p_\theta(\cdot | x)$, we assume the reparameterization $\hat{c} = \mu_\theta(x, \varepsilon)$ with $\varepsilon \sim \nu$ independent of θ . The map μ_θ is continuously differentiable in θ with $\|\nabla_\theta \mu_\theta(x, \varepsilon)\| \leq G_\mu$ almost surely for all $\theta \in \mathbb{R}^{d_\theta}$ and $x \in \mathcal{X}$, and there exists $L_\mu < \infty$ such that $\|\nabla_\theta \mu_\theta(x, \varepsilon) - \nabla_{\theta'} \mu_{\theta'}(x, \varepsilon)\| \leq L_\mu \|\theta - \theta'\|$ almost surely.

Corollary B.1 (Bounded and Lipschitz mean-decision gradient). Under Assumptions 2 and 3, $\theta \mapsto w_\theta^*(x)$ is differentiable for every $x \in \mathcal{X}$, with the score function representation

$$\nabla_\theta w_\theta^*(x) = \mathbb{E}_{\hat{c} \sim p_\theta(\cdot | x)}[w^*(\hat{c}) \nabla_\theta \log p_\theta(\hat{c} | x)^\top]. \quad (13)$$

Moreover, the Jacobian satisfies the bound

$$\|\nabla_\theta w_\theta^*(x)\| \leq B_{\nabla w_\theta^*} := B_S M, \quad \forall \theta \in \mathbb{R}^{d_\theta}, x \in \mathcal{X}, \quad (14)$$

and is L_w -Lipschitz in θ with $L_w := B_S M_\nabla$:

$$\|\nabla_\theta w_\theta^*(x) - \nabla_{\theta'} w_{\theta'}^*(x)\| \leq L_w \|\theta - \theta'\|, \quad \forall \theta, \theta' \in \mathbb{R}^{d_\theta}, x \in \mathcal{X}. \quad (15)$$

Proof. Under Assumption 3, dominated convergence applied to $w_\theta^*(x) = \int w^*(\hat{c}) p_\theta(\hat{c} | x) d\hat{c}$ yields

$$\nabla_\theta w_\theta^*(x) = \int w^*(\hat{c}) \nabla_\theta p_\theta(\hat{c} | x) d\hat{c} = \mathbb{E}_{\hat{c} \sim p_\theta(\cdot | x)} [w^*(\hat{c}) \nabla_\theta \log p_\theta(\hat{c} | x)^\top],$$

where the second equality uses the log-derivative identity $\nabla_\theta p_\theta = p_\theta \nabla_\theta \log p_\theta$.

Boundedness. Applying the triangle inequality to (13) in integral form, together with $\|w^*(\hat{c})\| \leq B_S$ (Assumption 2) and (11),

$$\|\nabla_\theta w_\theta^*(x)\| \leq \int \|w^*(\hat{c})\| \|\nabla_\theta p_\theta(\hat{c} | x)\| d\hat{c} \leq B_S \int \|\nabla_\theta p_\theta(\hat{c} | x)\| d\hat{c} \leq B_S M,$$

Lipschitz continuity. Subtracting the integral representations at θ and θ' ,

$$\nabla_\theta w_\theta^*(x) - \nabla_{\theta'} w_{\theta'}^*(x) = \int w^*(\hat{c}) (\nabla_\theta p_\theta(\hat{c} | x) - \nabla_{\theta'} p_{\theta'}(\hat{c} | x))^\top d\hat{c}.$$

Applying the triangle inequality, $\|w^*(\hat{c})\| \leq B_S$, and (12) yields

$$\|\nabla_\theta w_\theta^*(x) - \nabla_{\theta'} w_{\theta'}^*(x)\| \leq B_S \int \|\nabla_\theta p_\theta(\hat{c} | x) - \nabla_{\theta'} p_{\theta'}(\hat{c} | x)\| d\hat{c} \leq B_S M_\nabla \|\theta - \theta'\|.$$

Setting $L_w := B_S M_\nabla$ yields (15). \square

C Online regret analysis of the nuisance estimator

The nuisance update can be analyzed as an online convex optimization problem independently of the policy sequence $\{\theta_t\}_{t=1}^T$. Rather than tracking the moving per-iteration minimizer $\phi_{\theta_t}^* = \arg \min_{\phi \in \Phi} \mathcal{R}_\theta(f_\phi)$, we compare against the best fixed $\phi^* \in \Phi$ in hindsight, a valid comparison since f^* is the universal minimizer of \mathcal{R}_θ for every θ simultaneously (Remark 2.1). To analyze the nuisance update via online convex optimization arguments, we make the following assumptions, standard in the OCO literature (Orabona, 2019).

Assumption 5 (Realizability). *There exists $\phi^* \in \Phi$ such that $f_{\phi^*} = f^*$ (so $f^* \in \mathcal{F}$ with an explicit parameter-space comparator).*

Assumption 6. (i) Φ is convex and compact with diameter $D_\Phi := \sup_{\phi, \phi' \in \Phi} \|\phi - \phi'\| < \infty$.

(ii) There exists $G_\mathcal{R} < \infty$ such that $\|\nabla_\phi \ell_t(\phi)\| \leq G_\mathcal{R}$ almost surely for all t and $\phi \in \Phi$.

(iii) There exists $\lambda > 0$ such that, for every $\theta \in \mathbb{R}^{d_\theta}$, $\nabla_\phi^2 \mathcal{R}_\theta(f_\phi) \succeq \lambda I_d$.

Assumption 6(i)–(ii) are standard online convex optimization assumptions, bounding the feasible set diameter and gradient magnitudes respectively. Assumption 6(iii) requires the nuisance objective to be strongly convex in ϕ , uniformly over θ ; this holds, for example, for linear nuisance classes under standard feature non-degeneracy conditions. We first restate Proposition 2.1 and give its proof.

Proposition C.1 (Nuisance regret). *Under Assumptions 5–6, for any sequence $\{\theta_t\}_{t=1}^T$ and any fixed comparator $\phi^* \in \Phi$:*

(i) With $\eta_t = D_\Phi / (G_\mathcal{R} \sqrt{T})$

$$\frac{1}{T} \sum_{t=1}^T \mathbb{E}[\mathcal{R}_{\theta_t}(f_{\phi_t}) - \mathcal{R}_{\theta_t}(f_{\phi^*})] \leq \frac{D_\Phi G_\mathcal{R}}{\sqrt{T}}$$

(ii) With $\eta_t = 1/(\lambda t)$

$$\frac{1}{T} \sum_{t=1}^T \mathbb{E}[\mathcal{R}_{\theta_t}(f_{\phi_t}) - \mathcal{R}_{\theta_t}(f_{\phi^*})] \leq \frac{G_\mathcal{R}^2 (1 + \log T)}{2\lambda T}$$

Proof. Both bounds follow from standard online convex optimization arguments (Orabona, 2019); we include the derivations for completeness. By non-expansiveness of the Euclidean projection Π_{Φ} and the update rule $\phi_{t+1} = \Pi_{\Phi}(\phi_t - \eta_t g_t)$,

$$\|\phi_{t+1} - \phi^*\|^2 \leq \|\phi_t - \eta_t g_t - \phi^*\|^2 = \|\phi_t - \phi^*\|^2 - 2\eta_t \langle g_t, \phi_t - \phi^* \rangle + \eta_t^2 \|g_t\|^2 \quad (16)$$

Taking expectations, using unbiasedness of g_t and convexity of \mathcal{R}_{θ_t} in ϕ ,

$$\mathbb{E}[\langle \nabla_{\phi} \mathcal{R}_{\theta_t}(f_{\phi_t}), \phi_t - \phi^* \rangle] \geq \mathbb{E}[\mathcal{R}_{\theta_t}(f_{\phi_t}) - \mathcal{R}_{\theta_t}(f_{\phi^*})]$$

Substituting into (16) and rearranging,

$$2\eta_t \mathbb{E}[\mathcal{R}_{\theta_t}(f_{\phi_t}) - \mathcal{R}_{\theta_t}(f_{\phi^*})] \leq \mathbb{E}[\|\phi_t - \phi^*\|^2] - \mathbb{E}[\|\phi_{t+1} - \phi^*\|^2] + \eta_t^2 G_{\mathcal{R}}^2$$

Summing over $t = 1, \dots, T$, using a constant step-size $\eta_t = \eta$ and telescoping,

$$2\eta \sum_{t=1}^T \mathbb{E}[\mathcal{R}_{\theta_t}(f_{\phi_t}) - \mathcal{R}_{\theta_t}(f_{\phi^*})] \leq D_{\Phi}^2 + \eta^2 G_{\mathcal{R}}^2 T$$

Setting $\eta = D_{\Phi}/(G_{\mathcal{R}}\sqrt{T})$ yields the claimed bound. The bound (ii) follows from standard strong-convexity arguments in online convex optimization. When \mathcal{R}_{θ_t} is λ -strongly convex in ϕ ,

$$\mathbb{E}[\mathcal{R}_{\theta_t}(f_{\phi_t}) - \mathcal{R}_{\theta_t}(f_{\phi^*})] \leq \mathbb{E}[\langle g_t, \phi_t - \phi^* \rangle] - \frac{\lambda}{2} \mathbb{E}[\|\phi_t - \phi^*\|^2] \quad (17)$$

Non-expansiveness of Π_{Φ} gives $\mathbb{E}[\langle g_t, \phi_t - \phi^* \rangle] \leq \frac{1}{2\eta_t} (\mathbb{E}[\|\phi_t - \phi^*\|^2] - \mathbb{E}[\|\phi_{t+1} - \phi^*\|^2]) + \frac{\eta_t G_{\mathcal{R}}^2}{2}$. Substituting into (17) and choosing $\eta_t = 1/(\lambda t)$,

$$\mathbb{E}[\mathcal{R}_{\theta_t}(f_{\phi_t}) - \mathcal{R}_{\theta_t}(f_{\phi^*})] \leq \frac{\lambda(t-1)}{2} \mathbb{E}[\|\phi_t - \phi^*\|^2] - \frac{\lambda t}{2} \mathbb{E}[\|\phi_{t+1} - \phi^*\|^2] + \frac{G_{\mathcal{R}}^2}{2\lambda t}$$

Summing telescopes the distance terms (with non-positive boundary contribution), giving $\sum_{t=1}^T \mathbb{E}[\mathcal{R}_{\theta_t}(f_{\phi_t}) - \mathcal{R}_{\theta_t}(f_{\phi^*})] \leq \frac{G_{\mathcal{R}}^2(1+\log T)}{2\lambda}$. Dividing by T completes the proof. \square

D Convergence analysis: plug-in hybrid variant

The nuisance regret translates into a bound on the gradient bias by combining strong convexity of $\mathcal{R}_{\theta}(\cdot)$ with the Lipschitz parameterization of $f_{\phi}(\cdot)$. We define the plug-in bias as

$$B(\phi, \theta) := J(\phi, \theta) - V^{\text{cost}}(\theta).$$

Under realizability (Assumption 5)

$$V^{\text{cost}}(\theta) = J(\phi^*, \theta)$$

so equivalently

$$B(\phi, \theta) = J(\phi, \theta) - J(\phi^*, \theta)$$

Assumption 7. *The nuisance estimator function class is bounded and $L_{f_{\phi}}$ -Lipschitz, i.e., there exists $B_{f_{\phi}} < \infty$ such that $\|f_{\phi}(x)\| \leq B_{f_{\phi}}$ and $\|f_{\phi}(x) - f_{\phi'}(x)\| \leq L_{f_{\phi}} \|\phi - \phi'\|$ for all $\phi \in \Phi$ and $x \in \mathcal{X}$.*

Lemma D.1 (Regularity of J). *Under Assumptions 2,7 and Corollary B.1, the plug-in policy objective $J(\phi, \theta)$ satisfies:*

- (i) $\|\nabla_{\theta} J(\phi, \theta)\| \leq G^J := B_{f_{\phi}} B_{\nabla w_{\theta}^*}$;
- (ii) $\|\nabla_{\theta} J(\phi, \theta) - \nabla_{\theta} J(\phi, \theta')\| \leq L_{\theta}^J \|\theta - \theta'\|$ with $L_{\theta}^J := B_{f_{\phi}} L_w = B_{f_{\phi}} B_S M_{\nabla}$;
- (iii) $|J(\phi, \theta) - J(\phi', \theta)| \leq L_{\phi}^J \|\phi - \phi'\|$ with $L_{\phi}^J := B_S L_{f_{\phi}}$.

Proof. Part (i). Differentiating under the expectation, $\nabla_{\theta} J(\phi, \theta) = \mathbb{E}_x[(\nabla_{\theta} w_{\theta}^*(x))^{\top} f_{\phi}(x)]$, so $\|\nabla_{\theta} J(\phi, \theta)\| \leq \mathbb{E}_x[\|\nabla_{\theta} w_{\theta}^*(x)\| \|f_{\phi}(x)\|] \leq B_{\nabla w_{\theta}^*} B_{f_{\phi}}$, where the last step uses Corollary B.1 and Assumption 7.

Part (ii). For any $\theta, \theta' \in \mathbb{R}^{d_\theta}$,

$$\begin{aligned} \|\nabla_\theta J(\phi, \theta) - \nabla_\theta J(\phi, \theta')\| &\leq \mathbb{E}_x [\|f_\phi(x)\| \|\nabla_\theta w_\theta^*(x) - \nabla_\theta w_{\theta'}^*(x)\|] \\ &\leq B_{f_\phi} L_w \|\theta - \theta'\| \end{aligned}$$

where the second inequality uses Assumption 7 and the Lipschitz property of $\theta \mapsto \nabla_\theta w_\theta^*(x)$ established in Corollary B.1.

Part (iii). For any $\phi, \phi' \in \Phi$,

$$|J(\phi, \theta) - J(\phi', \theta)| \leq \mathbb{E}_x [\|f_\phi(x) - f_{\phi'}(x)\| \|w_\theta^*(x)\|] \leq B_S L_{f_\phi} \|\phi - \phi'\|.$$

□

Proposition D.2 (Averaged bias gradient). *Under Assumptions 5,6,7, and Corollary B.1,*

(i) With $\eta_t = D_\Phi / (G_{\mathcal{R}} \sqrt{T})$,

$$\frac{1}{T} \sum_{t=1}^T \mathbb{E}[\|\nabla_\theta B(\phi_t, \theta_t)\|^2] \leq \frac{2B_{\nabla w_\theta^*}^2 L_{f_\phi}^2 D_\Phi G_{\mathcal{R}}}{\lambda \sqrt{T}}$$

(ii) With $\eta_t = 1/(\lambda t)$,

$$\frac{1}{T} \sum_{t=1}^T \mathbb{E}[\|\nabla_\theta B(\phi_t, \theta_t)\|^2] \leq \frac{B_{\nabla w_\theta^*}^2 L_{f_\phi}^2 G_{\mathcal{R}}^2 (1 + \log T)}{\lambda^2 T}$$

Proof. Since $B(\phi, \theta) = J(\phi, \theta) - J(\phi^*, \theta)$ by Assumption 5, then

$$\nabla_\theta B(\phi_t, \theta_t) = \mathbb{E}_x [(\nabla_\theta w_{\theta_t}^*(x))^\top (f_{\phi_t}(x) - f^*(x))].$$

By Jensen's inequality, Cauchy-Schwarz, Corollary B.1, and the Lipschitz parameterization (Assumption 7)

$$\|\nabla_\theta B(\phi_t, \theta_t)\|^2 \leq B_{\nabla w_\theta^*}^2 \mathbb{E}_x [\|f_{\phi_t}(x) - f^*(x)\|^2] \leq B_{\nabla w_\theta^*}^2 L_{f_\phi}^2 \|\phi_t - \phi^*\|^2.$$

Under Assumption 5, f^* minimizes $\mathcal{R}_\theta(f)$ for every θ (Remark 2.1). Combined with λ -strong convexity (Assumption 6(iii)), this yields the quadratic-growth inequality

$$\frac{\lambda}{2} \|\phi_t - \phi^*\|^2 \leq \mathcal{R}_{\theta_t}(f_{\phi_t}) - \mathcal{R}_{\theta_t}(f^*). \quad (18)$$

Combining the previous bound with (18) yields

$$\|\nabla_\theta B(\phi_t, \theta_t)\|^2 \leq \frac{2B_{\nabla w_\theta^*}^2 L_{f_\phi}^2}{\lambda} (\mathcal{R}_{\theta_t}(f_{\phi_t}) - \mathcal{R}_{\theta_t}(f^*)).$$

Averaging over $t = 1, \dots, T$ and applying Proposition 2.1 yields the two stated bounds. □

The hybrid gradient is conditionally biased, but only through the nuisance error, as the following identity formalizes.

Lemma D.3 (Hybrid gradient bias). *Under Assumptions 2,3,5, and the log-derivative identity for g_t^{score} ,*

$$\mathbb{E}[g_t^\alpha \mid \phi_t, \theta_t] = \nabla_\theta V^{\text{cost}}(\theta_t) + (1 - \alpha) \nabla_\theta B(\phi_t, \theta_t) \quad (19)$$

Proof. By Assumption 3 and dominated convergence, we may exchange differentiation and expectation:

$$\nabla_\theta V^{\text{cost}}(\theta_t) = \mathbb{E}_{x, \hat{c}} [c^\top w^*(\hat{c}) \nabla_\theta \log p_{\theta_t}(\hat{c} \mid x)] = \mathbb{E}[g_t^{\text{score}} \mid \phi_t, \theta_t],$$

where the second equality uses $w_t = w^*(\hat{c}_t)$ and $y_t = c_t^\top w_t$.

For the plug-in estimator, since $w_t = w^*(\hat{c}_t)$ and applying the log-derivative identity,

$$\begin{aligned} \mathbb{E}[g_t^{\text{plug-in}} \mid \phi_t, \theta_t] &= \mathbb{E}_{x, \hat{c}} [(w^*(\hat{c})^\top f_{\phi_t}(x)) \nabla_\theta \log p_{\theta_t}(\hat{c} \mid x)] \\ &= \mathbb{E}_x [f_{\phi_t}(x)^\top \mathbb{E}_{\hat{c}} [w^*(\hat{c}) \nabla_\theta \log p_{\theta_t}(\hat{c} \mid x)^\top]] \\ &= \mathbb{E}_x [f_{\phi_t}(x)^\top \nabla_\theta w_{\theta_t}^*(x)] = \nabla_\theta J(\phi_t, \theta_t), \end{aligned}$$

using Corollary B.1 for the third equality. Combining the two by linearity of expectation yields the claim. □

Assumption 8 (Gradient variances). *There exist $\sigma_{\text{score}}, \sigma_{\text{plug-in}} < \infty$ such that:*

$$\text{Var}[g_t^{\text{score}} | \phi_t, \theta_t] \leq \sigma_{\text{score}}^2, \quad \text{Var}[g_t^{\text{plug-in}} | \phi_t, \theta_t] \leq \sigma_{\text{plug-in}}^2.$$

Lemma D.4 (One-Step Descent). *Under Assumptions 5–8, the iterates of the policy update satisfy*

$$\begin{aligned} \mathbb{E}[V^{\text{cost}}(\theta_{t+1})] &\leq \mathbb{E}[V^{\text{cost}}(\theta_t)] - \frac{\beta}{2} \mathbb{E}[\|\nabla_{\theta} V^{\text{cost}}(\theta_t)\|^2] \\ &\quad + \frac{\beta(1-\alpha)^2}{2} \mathbb{E}[\|\nabla_{\theta} B(\phi_t, \theta_t)\|^2] + \frac{L_{\theta}^J \beta^2}{2} ((G^J)^2 + \sigma_{\alpha}^2). \end{aligned} \quad (20)$$

with $\sigma_{\alpha}^2 := (\alpha\sigma_{\text{score}} + (1-\alpha)\sigma_{\text{plug-in}})^2$.

Proof of Lemma D.4. Since $V^{\text{cost}}(\theta) = J(\phi^*, \theta)$ is L_{θ}^J -smooth in θ (Lemma D.1(ii)), the descent lemma applied to the update $\theta_{t+1} = \theta_t - \beta g_t^{\alpha}$ gives

$$V^{\text{cost}}(\theta_{t+1}) \leq V^{\text{cost}}(\theta_t) + \langle \nabla_{\theta} V^{\text{cost}}(\theta_t), \theta_{t+1} - \theta_t \rangle + \frac{L_{\theta}^J}{2} \|\theta_{t+1} - \theta_t\|^2 \quad (21)$$

Substituting $\theta_{t+1} - \theta_t = -\beta g_t^{\alpha}$ and taking conditional expectation given (ϕ_t, θ_t) ,

$$\mathbb{E}[\langle \nabla_{\theta} V^{\text{cost}}(\theta_t), -\beta g_t^{\alpha} \rangle | \phi_t, \theta_t] = -\beta \langle \nabla_{\theta} V^{\text{cost}}(\theta_t), \mathbb{E}[g_t^{\alpha} | \phi_t, \theta_t] \rangle$$

Applying Lemma D.3, $\mathbb{E}[g_t^{\alpha} | \phi_t, \theta_t] = \nabla_{\theta} V^{\text{cost}}(\theta_t) + (1-\alpha)\nabla_{\theta} B(\phi_t, \theta_t)$, so

$$-\beta \langle \nabla_{\theta} V^{\text{cost}}, \nabla_{\theta} V^{\text{cost}} + (1-\alpha)\nabla_{\theta} B \rangle = -\beta \|\nabla_{\theta} V^{\text{cost}}\|^2 - \beta \langle \nabla_{\theta} V^{\text{cost}}, (1-\alpha)\nabla_{\theta} B \rangle$$

Applying the inequality $-\langle a, b \rangle \leq \frac{1}{2}\|a\|^2 + \frac{1}{2}\|b\|^2$ to the cross term,

$$\mathbb{E}[\langle \nabla_{\theta} V^{\text{cost}}, -\beta g_t^{\alpha} \rangle | \phi_t, \theta_t] \leq -\frac{\beta}{2} \|\nabla_{\theta} V^{\text{cost}}(\theta_t)\|^2 + \frac{\beta(1-\alpha)^2}{2} \|\nabla_{\theta} B(\phi_t, \theta_t)\|^2 \quad (22)$$

We bound $\mathbb{E}[\|g_t^{\alpha}\|^2 | \phi_t, \theta_t]$ using the bias-variance decomposition

$$\mathbb{E}[\|g_t^{\alpha}\|^2 | \phi_t, \theta_t] = \text{Var}[g_t^{\alpha} | \phi_t, \theta_t] + \|\mathbb{E}[g_t^{\alpha} | \phi_t, \theta_t]\|^2 \quad (23)$$

For the variance term, write $g_t^{\alpha} = \alpha g_t^{\text{score}} + (1-\alpha)g_t^{\text{plug-in}}$. Expanding,

$$\begin{aligned} \text{Var}[g_t^{\alpha} | \phi_t, \theta_t] &= \alpha^2 \text{Var}[g_t^{\text{score}} | \phi_t, \theta_t] + (1-\alpha)^2 \text{Var}[g_t^{\text{plug-in}} | \phi_t, \theta_t] \\ &\quad + 2\alpha(1-\alpha) \text{Cov}[g_t^{\text{score}}, g_t^{\text{plug-in}} | \phi_t, \theta_t] \end{aligned}$$

We bound the covariance term via Cauchy-Schwarz

$$|\text{Cov}[g_t^{\text{score}}, g_t^{\text{plug-in}} | \phi_t, \theta_t]| \leq \sigma_{\text{score}} \sigma_{\text{plug-in}}$$

where the second inequality uses Assumption 8. Substituting and completing the square,

$$\text{Var}[g_t^{\alpha} | \phi_t, \theta_t] \leq (\alpha\sigma_{\text{score}} + (1-\alpha)\sigma_{\text{plug-in}})^2 =: \sigma_{\alpha}^2 \quad (24)$$

For the squared mean term, by Lemma D.3, the triangle inequality, $\|\mathbb{E}[g_t^{\alpha} | \phi_t, \theta_t]\| \leq \alpha\|\nabla_{\theta} V^{\text{cost}}(\theta_t)\| + (1-\alpha)\|\nabla_{\theta} J(\phi_t, \theta_t)\| = \alpha\|\nabla_{\theta} J(\phi^*, \theta_t)\| + (1-\alpha)\|\nabla_{\theta} J(\phi_t, \theta_t)\| \leq G^J$ where the last inequality is given by Lemma D.1. Substituting into (23),

$$\mathbb{E}[\|g_t^{\alpha}\|^2 | \phi_t, \theta_t] \leq \sigma_{\alpha}^2 + (G^J)^2 \quad (25)$$

Substituting (22) and (25) into (21) and taking full expectations,

$$\begin{aligned} \mathbb{E}[V^{\text{cost}}(\theta_{t+1})] &\leq \mathbb{E}[V^{\text{cost}}(\theta_t)] - \frac{\beta}{2} \mathbb{E}[\|\nabla_{\theta} V^{\text{cost}}(\theta_t)\|^2] \\ &\quad + \frac{\beta(1-\alpha)^2}{2} \mathbb{E}[\|\nabla_{\theta} B(\phi_t, \theta_t)\|^2] + \frac{L_{\theta}^J \beta^2}{2} (\sigma_{\alpha}^2 + (G^J)^2) \end{aligned}$$

which is the claimed inequality. \square

We are now in a position to state Theorem 2.2 with explicit constants and provide its proof. The result follows directly by combining the one-step descent inequality (Lemma D.4) with the averaged bias bound of Proposition D.2.

Theorem D.5 (Non-convex stationarity, plug-in variant). *Let $V^* := \inf_{\theta} V^{\text{cost}}(\theta) > -\infty$ Under Assumptions 2–8, with step size $\beta = 1/(L_{\theta}^J \sqrt{T})$, Algorithm 1 satisfies,*

$$\frac{1}{T} \sum_{t=1}^T \mathbb{E}[\|\nabla_{\theta} V^{\text{cost}}(\theta_t)\|^2] \leq \frac{2L_{\theta}^J \Delta_1 + (G^J)^2 + \sigma_{\alpha}^2}{\sqrt{T}} + (1-\alpha)^2 B_{\nabla w_{\theta}^*}^2 L_{f_{\phi}}^2 \cdot \mathcal{B}_{\text{bias}}(T), \quad (26)$$

where $\Delta_1 := V^{\text{cost}}(\theta_1) - V^*$, and the bias decay $\mathcal{B}_{\text{bias}}(T)$ depends on the nuisance step size:

(i) With $\eta_t = D_{\Phi}/(G_{\mathcal{R}} \sqrt{T})$: $\mathcal{B}_{\text{bias}}(T) = \frac{2D_{\Phi} G_{\mathcal{R}}}{\lambda \sqrt{T}}$.

(ii) With $\eta_t = 1/(\lambda t)$: $\mathcal{B}_{\text{bias}}(T) = \frac{G_{\mathcal{R}}^2 (1 + \log T)}{\lambda^2 T}$.

Proof. Rearranging Lemma D.4,

$$\begin{aligned} \frac{\beta}{2} \mathbb{E}[\|\nabla_{\theta} V^{\text{cost}}(\theta_t)\|^2] &\leq \mathbb{E}[V^{\text{cost}}(\theta_t)] - \mathbb{E}[V^{\text{cost}}(\theta_{t+1})] \\ &\quad + \frac{\beta(1-\alpha)^2}{2} \mathbb{E}[\|\nabla_{\theta} B(\phi_t, \theta_t)\|^2] + \frac{L_{\theta}^J \beta^2}{2} ((G^J)^2 + \sigma_{\alpha}^2) \end{aligned}$$

Summing over $t = 1, \dots, T$ and using $\mathbb{E}[V^{\text{cost}}(\theta_{T+1})] \geq V^*$,

$$\frac{\beta}{2} \sum_{t=1}^T \mathbb{E}[\|\nabla_{\theta} V^{\text{cost}}(\theta_t)\|^2] \leq V^{\text{cost}}(\theta_1) - V^* + \frac{\beta(1-\alpha)^2}{2} \sum_{t=1}^T \mathbb{E}[\|\nabla_{\theta} B\|^2] + \frac{L_{\theta}^J \beta^2 T}{2} ((G^J)^2 + \sigma_{\alpha}^2)$$

Dividing by $\beta T/2$ and setting $\beta = 1/(L_{\theta}^J \sqrt{T})$,

$$\frac{1}{T} \sum_{t=1}^T \mathbb{E}[\|\nabla_{\theta} V^{\text{cost}}(\theta_t)\|^2] \leq \frac{2L_{\theta}^J (V^{\text{cost}}(\theta_1) - V^*) + (G^J)^2 + \sigma_{\alpha}^2}{\sqrt{T}} + (1-\alpha)^2 \frac{1}{T} \sum_{t=1}^T \mathbb{E}[\|\nabla_{\theta} B\|^2]$$

Applying Proposition D.2(i)-(ii) yields the results. \square

E Convergence analysis: surrogate hybrid variant

This appendix extends the hybrid gradient framework to the surrogate setting, where the plug-in policy gradient is replaced by a differentiable proxy. A *surrogate cost function* $h^{\text{sur}} : \mathbb{R}^{d_w} \times \mathbb{R}^{d_w} \rightarrow \mathbb{R}$ replaces the inner objective $c^{\top} w^*(\hat{c})$ with a smooth, globally defined surrogate.

For a given policy θ , the plug-in surrogate objective is defined in Equation 6

$$J^{\text{sur}}(\phi, \theta) := \mathbb{E}_x [\mathbb{E}_{\hat{c} \sim p_{\theta}(\cdot|x)} [h^{\text{sur}}(f_{\phi}(x), \hat{c})]]$$

Realizability (Assumption 5) implies $V^{\text{cost}}(\theta) = J(\phi^*, \theta)$ as an exact identity, reducing the problem to the plug-in objective $J(\phi, \theta)$ and its surrogate $J^{\text{sur}}(\phi, \theta)$. Our analysis therefore takes $J^{\text{sur}}(\phi^*, \theta)$ directly as the surrogate target.

The surrogate nuisance bias is entirely captured by the surrogate analog:

$$B^{\text{sur}}(\phi, \theta) := J^{\text{sur}}(\phi, \theta) - J^{\text{sur}}(\phi^*, \theta).$$

The bias vanishes when $f_{\phi} = f^*$, isolating the contribution of nuisance error. Whenever the surrogate is faithful and ϕ is close to ϕ^* , a good policy under $J^{\text{sur}}(\phi, \cdot)$ remains good under $J(\phi, \cdot)$, and therefore under V^{cost} .

Assumption 9 (Surrogate regularity). *The surrogate $h^{\text{sur}}(c, \hat{c})$ satisfies:*

- (i) $\hat{c} \mapsto h^{\text{sur}}(c, \hat{c})$ is continuously differentiable for every $c \in \mathbb{R}^{d_w}$, and there exists $G_{\text{sur}} < \infty$ such that $\|\nabla_{\hat{c}} h^{\text{sur}}(c, \hat{c})\| \leq G_{\text{sur}}$ almost surely.

- (ii) There exist $L_c^{\text{sur}}, L_{\hat{c}}^{\text{sur}} < \infty$ such that for all $c, c', \hat{c}, \hat{c}' \in \mathbb{R}^{d_w}$,
- $$\begin{aligned} \|\nabla_{\hat{c}} h^{\text{sur}}(c, \hat{c}) - \nabla_{\hat{c}} h^{\text{sur}}(c', \hat{c})\| &\leq L_c^{\text{sur}} \|c - c'\|, \\ \|\nabla_{\hat{c}} h^{\text{sur}}(c, \hat{c}) - \nabla_{\hat{c}} h^{\text{sur}}(c, \hat{c}')\| &\leq L_{\hat{c}}^{\text{sur}} \|\hat{c} - \hat{c}'\|. \end{aligned}$$

To construct a tractable estimator of $\nabla_{\theta} J^{\text{sur}}$ we assume that $p_{\theta}(\cdot | x)$ admits a reparameterization $\hat{c} = \mu_{\theta}(x, \varepsilon)$ with $\varepsilon \sim \nu$ independent of θ (Assumption 4). At iteration t , having sampled $\varepsilon_t \sim \nu$ and computed $\hat{c}_t = \mu_{\theta_t}(x_t, \varepsilon_t)$, the chain rule yields the surrogate gradient estimator

$$g_t^{\text{sur}} := (\nabla_{\theta} \mu_{\theta_t}(x_t, \varepsilon_t))^{\top} \nabla_{\hat{c}} h^{\text{sur}}(f_{\phi_t}(x_t), \hat{c}_t)$$

Proposition E.1 (Unbiasedness of g_t^{sur}). *Under Assumptions 4 and 9,*

$$\mathbb{E}[g_t^{\text{sur}} | \phi_t, \theta_t] = \nabla_{\theta} J^{\text{sur}}(\phi_t, \theta_t)$$

Proof. By Assumption 4, $\hat{c}_t = \mu_{\theta_t}(x_t, \varepsilon_t)$ with $\varepsilon_t \sim \nu$ independent of θ_t , so the reparameterization trick and Assumptions 9(i) and 4 justify exchanging differentiation and expectation:

$$\nabla_{\theta} J^{\text{sur}}(\phi_t, \theta_t) = \mathbb{E}_{x, \varepsilon} \left[(\nabla_{\theta} \mu_{\theta_t}(x, \varepsilon))^{\top} \nabla_{\hat{c}} h^{\text{sur}}(f_{\phi_t}(x), \mu_{\theta_t}(x, \varepsilon)) \right] = \mathbb{E}[g_t^{\text{sur}} | \phi_t, \theta_t]. \quad \square$$

The surrogate hybrid gradient estimator is $g_t^{\alpha, \text{sur}} := \alpha g_t^{\text{score}} + (1 - \alpha) g_t^{\text{sur}}$.

We operate under the same regime as the plug-in policy case. Define the target objective

$$V^{\alpha}(\theta) := \alpha V^{\text{cost}}(\theta) + (1 - \alpha) J^{\text{sur}}(\phi^*, \theta) \quad (27)$$

let $\tilde{G}_{\alpha} := \alpha G^J + (1 - \alpha) G_{\text{sur}}$ bound the norm of $\mathbb{E}[g_t^{\alpha, \text{sur}} | \phi_t, \theta_t]$.

Assumption 10 (Surrogate gradient moments). *There exist $\sigma_{\text{sur}} < \infty$ such that $\text{Var}[g_t^{\text{sur}} | \phi_t, \theta_t] \leq \sigma_{\text{sur}}^2$.*

Assumption 11 (Surrogate gradient norm bound). *There exists $G_{\text{sur}}^J < \infty$ such that $\|\nabla_{\theta} J^{\text{sur}}(\phi, \theta)\| \leq G_{\text{sur}}^J$ for all $\phi \in \Phi$, $\theta \in \mathbb{R}^{d_{\theta}}$. Under Assumptions 4–9, this holds with $G_{\text{sur}}^J := G_{\mu} G_{\text{sur}}$.*

Lemma E.2 (Surrogate hybrid gradient bias). *Under Assumptions 2,3,4,5,9 and the log-derivative identity for g_t^{score} ,*

$$\mathbb{E}[g_t^{\alpha, \text{sur}} | \phi_t, \theta_t] = \nabla_{\theta} V^{\alpha}(\theta_t) + (1 - \alpha) \nabla_{\theta} B^{\text{sur}}(\phi_t, \theta_t)$$

Proof. By the log-derivative identity, $\mathbb{E}[g_t^{\text{score}} | \phi_t, \theta_t] = \nabla_{\theta} V^{\text{cost}}(\theta_t)$. Unbiasedness of the reparameterization estimator gives $\mathbb{E}[g_t^{\text{sur}} | \phi_t, \theta_t] = \nabla_{\theta} J^{\text{sur}}(\phi_t, \theta_t) = \nabla_{\theta} J^{\text{sur}}(\phi^*, \theta_t) + \nabla_{\theta} B^{\text{sur}}(\phi_t, \theta_t)$. Linearity of expectation yields the claim. \square

Lemma E.3 (Smoothness of V^{α}). *Under Assumptions 5,9 and 4, $J^{\text{sur}}(\phi^*, \cdot)$ is L_{θ}^{sur} -smooth. Consequently V^{α} is L_{θ}^{α} -smooth with $L_{\theta}^{\alpha} := \alpha L_{\theta}^J + (1 - \alpha) L_{\theta}^{\text{sur}}$.*

Proof. We show $J^{\text{sur}}(\phi^*, \cdot)$ is L_{θ}^{sur} -smooth, the smoothness of V^{α} then follows because a convex combination of smooth functions is smooth. By Assumption 4, we may write

$$\nabla_{\theta} J^{\text{sur}}(\phi^*, \theta) = \mathbb{E}_{x, \varepsilon} \left[(\nabla_{\theta} \mu_{\theta}(x, \varepsilon))^{\top} \nabla_{\hat{c}} h^{\text{sur}}(f^*(x), \mu_{\theta}(x, \varepsilon)) \right].$$

For any $\theta, \theta' \in \mathbb{R}^{d_{\theta}}$, denote $\hat{c} = \mu_{\theta}(x, \varepsilon)$ and $\hat{c}' = \mu_{\theta'}(x, \varepsilon)$. Adding and subtracting $(\nabla_{\theta} \mu_{\theta'}(x, \varepsilon))^{\top} \nabla_{\hat{c}} h^{\text{sur}}(f^*(x), \hat{c}')$ and applying the triangle inequality,

$$\begin{aligned} &\|\nabla_{\theta} J^{\text{sur}}(\phi^*, \theta) - \nabla_{\theta} J^{\text{sur}}(\phi^*, \theta')\| \\ &\leq \mathbb{E}_{x, \varepsilon} [\|\nabla_{\theta} \mu_{\theta}(x, \varepsilon) - \nabla_{\theta} \mu_{\theta'}(x, \varepsilon)\| \|\nabla_{\hat{c}} h^{\text{sur}}(f^*(x), \hat{c})\|] \\ &\quad + \mathbb{E}_{x, \varepsilon} [\|\nabla_{\theta} \mu_{\theta'}(x, \varepsilon)\| \|\nabla_{\hat{c}} h^{\text{sur}}(f^*(x), \hat{c}) - \nabla_{\hat{c}} h^{\text{sur}}(f^*(x), \hat{c}')\|] \\ &\leq L_{\mu} G_{\text{sur}} \|\theta - \theta'\| + G_{\mu} L_{\hat{c}}^{\text{sur}} \mathbb{E}_{x, \varepsilon} [\|\hat{c} - \hat{c}'\|] \\ &\leq (L_{\mu} G_{\text{sur}} + G_{\mu}^2 L_{\hat{c}}^{\text{sur}}) \|\theta - \theta'\|, \end{aligned}$$

where the second inequality uses Assumption 4 ($\|\nabla_{\theta} \mu\| \leq G_{\mu}$, L_{μ} -Lipschitz) and Assumption 9(i)-(ii); the third inequality uses $\|\hat{c} - \hat{c}'\| = \|\mu_{\theta}(x, \varepsilon) - \mu_{\theta'}(x, \varepsilon)\| \leq G_{\mu} \|\theta - \theta'\|$ from Assumption 4. Setting $L_{\theta}^{\text{sur}} := L_{\mu} G_{\text{sur}} + G_{\mu}^2 L_{\hat{c}}^{\text{sur}}$ proves smoothness of $J^{\text{sur}}(\phi^*, \cdot)$. Since $V^{\text{cost}} = J(\phi^*, \cdot)$ is L_{θ}^J -smooth (Lemma D.1(ii)) and V^{α} is a convex combination, V^{α} is L_{θ}^{α} -smooth with $L_{\theta}^{\alpha} := \alpha L_{\theta}^J + (1 - \alpha) L_{\theta}^{\text{sur}}$. \square

Proposition E.4 (Averaged surrogate bias gradient). *Under Assumptions 5–6,9–10, with step size $\eta_t = 1/(\lambda t)$ in the nuisance update,*

$$\frac{1}{T} \sum_{t=1}^T \mathbb{E}[\|\nabla_{\theta} B^{\text{sur}}(\phi_t, \theta_t)\|^2] \leq \frac{(L_c^{\text{sur}})^2 G_{\mu}^2 L_{f_{\phi}}^2 G_{\mathcal{R}}^2 (1 + \log T)}{\lambda^2 T} = \mathcal{O}\left(\frac{\log T}{T}\right)$$

Proof. Differentiating under the expectation (justified by Assumptions 9(i) and 4),

$$\nabla_{\theta} B^{\text{sur}}(\phi_t, \theta_t) = \mathbb{E}_{x, \varepsilon} \left[(\nabla_{\theta} \mu_{\theta_t}(x, \varepsilon))^{\top} (\nabla_{\hat{c}} h^{\text{sur}}(f_{\phi_t}(x), \hat{c}) - \nabla_{\hat{c}} h^{\text{sur}}(f^*(x), \hat{c})) \right]$$

Jensen's inequality, Cauchy-Schwarz, $\|\nabla_{\theta} \mu\| \leq G_{\mu}$, and Assumption 9(ii) give

$$\|\nabla_{\theta} B^{\text{sur}}(\phi_t, \theta_t)\|^2 \leq (L_c^{\text{sur}})^2 G_{\mu}^2 \mathbb{E}_x [\|f_{\phi_t}(x) - f^*(x)\|^2] \quad (28)$$

By strong convexity $\mathbb{E}_x [\|f_{\phi_t}(x) - f^*(x)\|^2] \leq \frac{2L_{f_{\phi}}^2}{\lambda} \mathbb{E}[\mathcal{R}_{\theta_t}(f_{\phi_t}) - \mathcal{R}_{\theta_t}(f^*)]$. Averaging (28) over t and applying Proposition 2.1(ii) yields the claim. \square

Lemma E.5 (One-Step Descent, Surrogate Variant). *Under Assumptions 5–6,9–10, the iterates of the hybrid update $\theta_{t+1} = \theta_t - \beta g_t^{\alpha, \text{sur}}$ satisfy*

$$\begin{aligned} \mathbb{E}[V^{\alpha}(\theta_{t+1})] - \mathbb{E}[V^{\alpha}(\theta_t)] &\leq -\frac{\beta}{2} \mathbb{E}[\|\nabla V^{\alpha}(\theta_t)\|^2] \\ &\quad + \frac{\beta(1-\alpha)^2}{2} \mathbb{E}[\|\nabla_{\theta} B^{\text{sur}}(\phi_t, \theta_t)\|^2] \\ &\quad + \frac{L_{\theta}^{\alpha} \beta^2}{2} (\tilde{G}_{\alpha}^2 + \tilde{\sigma}_{\alpha}^2). \end{aligned} \quad (29)$$

with $\tilde{\sigma}_{\alpha}^2 := (\alpha \sigma_{\text{score}} + (1-\alpha) \sigma_{\text{sur}})^2$ and $\tilde{G}_{\alpha} := \alpha G^J + (1-\alpha) G_{\text{sur}}^J$.

Proof. By Lemma E.3, V^{α} is L_{θ}^{α} -smooth, so the descent lemma yields

$$V^{\alpha}(\theta_{t+1}) \leq V^{\alpha}(\theta_t) + \langle \nabla V^{\alpha}(\theta_t), \theta_{t+1} - \theta_t \rangle + \frac{L_{\theta}^{\alpha}}{2} \|\theta_{t+1} - \theta_t\|^2$$

Substituting $\theta_{t+1} - \theta_t = -\beta g_t^{\alpha, \text{sur}}$ and taking conditional expectation given (ϕ_t, θ_t) , Lemma E.2 gives

$$\mathbb{E}[\langle \nabla V^{\alpha}, -\beta g_t^{\alpha, \text{sur}} \mid \phi_t, \theta_t \rangle] = -\beta \|\nabla V^{\alpha}(\theta_t)\|^2 - \beta \langle \nabla V^{\alpha}(\theta_t), (1-\alpha) \nabla_{\theta} B^{\text{sur}}(\phi_t, \theta_t) \rangle$$

Applying Young's inequality to the cross term,

$$\mathbb{E}[\langle \nabla V^{\alpha}, -\beta g_t^{\alpha, \text{sur}} \mid \phi_t, \theta_t \rangle] \leq -\frac{\beta}{2} \|\nabla V^{\alpha}(\theta_t)\|^2 + \frac{\beta(1-\alpha)^2}{2} \|\nabla_{\theta} B^{\text{sur}}(\phi_t, \theta_t)\|^2 \quad (30)$$

For the quadratic term, the bias-variance decomposition gives $\mathbb{E}[\|g_t^{\alpha, \text{sur}}\|^2 \mid \phi_t, \theta_t] = \text{Var}[g_t^{\alpha, \text{sur}} \mid \phi_t, \theta_t] + \|\mathbb{E}[g_t^{\alpha, \text{sur}} \mid \phi_t, \theta_t]\|^2$. By the same Cauchy-Schwarz argument as in the proof of Lemma D.4 (applied with σ_{sur} in place of $\sigma_{\text{plug-in}}$), and linearity of expectation

$$\text{Var}[g_t^{\alpha, \text{sur}} \mid \phi_t, \theta_t] \leq (\alpha \sigma_{\text{score}} + (1-\alpha) \sigma_{\text{sur}})^2 = \tilde{\sigma}_{\alpha}^2, \quad \|\mathbb{E}[g_t^{\alpha, \text{sur}} \mid \phi_t, \theta_t]\|^2 \leq \tilde{G}_{\alpha}^2$$

with $\tilde{G}_{\alpha} := \alpha G^J + (1-\alpha) G_{\text{sur}}^J$. Substituting into the descent lemma and taking full expectations gives (29). \square

We restate Theorem 2.3 with explicit constants. The result follows by the same argument as Theorem 2.2, replacing Lemma D.4 with Lemma E.5 and Proposition D.2 with Proposition E.4.

Theorem E.6 (Non-convex stationarity, surrogate variant). *Let $V^{\alpha, \star} := \inf_{\theta} V^{\alpha}(\theta)$ where $V^{\alpha}(\theta) := \alpha V^{\text{cost}}(\theta) + (1-\alpha) J^{\text{sur}}(\phi^{\star}, \theta)$. Running Algorithm 1 with $\beta = 1/(L_{\theta}^{\alpha} \sqrt{T})$ and $\eta_t = 1/(\lambda t)$ yields*

$$\frac{1}{T} \sum_{t=1}^T \mathbb{E}[\|\nabla V^{\alpha}(\theta_t)\|^2] \leq \frac{2L_{\theta}^{\alpha} \Delta_1^{\alpha} + \tilde{G}_{\alpha}^2 + \tilde{\sigma}_{\alpha}^2}{\sqrt{T}} + \frac{(1-\alpha)^2 (L_c^{\text{sur}})^2 G_{\mu}^2 L_{f_{\phi}}^2 G_{\mathcal{R}}^2 (1 + \log T)}{\lambda^2 T} \quad (31)$$

with $\Delta_1^{\alpha} = V^{\alpha}(\theta_1) - V^{\alpha, \star}$, $\tilde{\sigma}_{\alpha}^2 := (\alpha \sigma_{\text{score}} + (1-\alpha) \sigma_{\text{sur}})^2$ and $\tilde{G}_{\alpha} := \alpha G^J + (1-\alpha) G_{\text{sur}}^J$.

Proof of Theorem 2.3. Following the same proof as Theorem 2.2, rearranging Lemma E.5, summing over $t = 1, \dots, T$, telescoping, and using $\mathbb{E}[V^\alpha(\theta_{T+1})] \geq V^{\alpha,*}$,

$$\frac{\beta}{2} \sum_{t=1}^T \mathbb{E}[\|\nabla V^\alpha(\theta_t)\|^2] \leq V^\alpha(\theta_1) - V^{\alpha,*} + \frac{\beta(1-\alpha)^2}{2} \sum_{t=1}^T \mathbb{E}[\|\nabla_\theta B^{\text{sur}}\|^2] + \frac{L_\theta^\alpha \beta^2 T}{2} (\tilde{G}_\alpha^2 + \tilde{\sigma}_\alpha^2)$$

Dividing by $\beta T/2$, substituting $\beta = 1/(L_\theta^\alpha \sqrt{T})$, and applying Proposition E.4 yields (31). \square

F Benchmark data and generation details

Top- k instance. The default top- k configuration has $d = 15$ items, cardinality $k = 2$, and context dimension $p = 5$. Contexts are sampled i.i.d. according to $x_t \sim \mathcal{N}(0, I_p)$. At environment construction time, the generator draws and fixes a binary coefficient matrix $\omega_{\text{top}} \in \{0, 1\}^{d \times p}$ with i.i.d. Bernoulli(0.5) entries. Let deg denote the polynomial degree parameter and ξ the multiplicative-noise radius. At iteration t , it forms a latent vector $u_t \in \mathbb{R}^d$ as $u_t = [1 + (1 + \omega_{\text{top}} x_t / \sqrt{p})^{\text{deg}}] \odot \xi_t$, where $\xi_{t,j} \sim \text{Unif}[1 - \bar{\xi}, 1 + \bar{\xi}]$ when multiplicative noise is enabled, while $\xi_{t,j} = 1$ otherwise. The realized cost vector is then $c_t = -u_t$.

Shortest-path instance. The default shortest-path configuration has context dimension $p = 10$ and $q = 40$ edges over the fixed 5×5 right/down DAG described in Section 3.1. Contexts are sampled i.i.d. as $x_t \sim \mathcal{N}(0, I_p)$. The generator draws an independent binary coefficient matrix $\omega_{\text{sp}} \in \{0, 1\}^{q \times p}$ and forms $u_t \in \mathbb{R}^q$ by the same polynomial construction as in the top- k instance, with ω_{sp} replacing ω_{top} . The generated vector is used directly as the realized edge-cost vector, $c_t = u_t$.

Pricing instance. The default pricing configuration has $n = 20$ products, $K_{\text{price}} = 4$ normalized price levels in $[0.1, 0.9]$, promotion threshold $L_{\text{promo}} = 2$, and budget $B_{\text{promo}} = 10$. At environment initialization, each product i is assigned a fixed latent direction $b_i \in \mathbb{R}^p$, sampled once and row-normalized. At the beginning of period t , the context is drawn as $x_t \sim \mathcal{N}(0, I_p)$, with default $p = 25$. Let k_c and k_p control the context and price nonlinearities, with $k_c = k_p = \text{deg}$ in the paper experiments. For each product-price pair (i, ℓ) , the context-dependent mean demand is $\mu_{i\ell}(x_t) = \text{softplus}(|b_i^\top x_t|^{k_c} + (1 - \tilde{\pi}_\ell)^{k_p})$. The environment may additionally apply a centered common multiplicative shock with scale σ_{shock} , default $\sigma_{\text{shock}} = 0.1$, using $\zeta_t \sim \mathcal{N}(0, 1)$: $\tilde{\mu}_{i\ell,t} = \mu_{i\ell}(x_t) \exp(\sigma_{\text{shock}} \zeta_t - \frac{1}{2} \sigma_{\text{shock}}^2)$. Conditional on this perturbed mean, latent demand is sampled independently as $y_{i\ell,t} \sim \text{Poisson}(\tilde{\mu}_{i\ell,t})$ across product-price pairs. Letting $a_t(i) \in \{1, \dots, K_{\text{price}}\}$ denote the price level assigned to product i by action w_t , the realized revenue at period t is $r_t = \sum_{i=1}^n \tilde{\pi}_{a_t(i)} y_{i, a_t(i), t}$, and the bandit feedback is the realized cost $v_t = c_i^{\text{price}}(w_t, x_t)^\top w_t = -r_t$.

Energy-scheduling instance. The energy-scheduling benchmark of Section 3.1 follows the decision-focused learning benchmark suite of Mandi et al. (2024) and uses empirical day-level SEMO price data. The context is a 48×8 slot-feature matrix, and $\mathcal{J}, \mathcal{M}, \mathcal{U}, \mathcal{T}_{\text{slot}} = \{1, \dots, 48\}$ index tasks, machines, resources, and slots. With per-task power p_j and slot length δ_{slot} , the iteration- t cost vector $c_t \in \mathbb{R}^{d_w}$ of Section 3.1 has components $c_{jms,t} := p_j \delta_{\text{slot}} \sum_{s'=s}^{s+d_j-1} \pi_{t,s'}^*$, giving the energy cost of task j when started on machine m at slot s under price profile π_t^* . The scheduling instance is fixed within a run, with feasible start-slot sets $\mathcal{T}_j = \{s : a_j \leq s, s + d_j - 1 \leq b_j\}$ given by per-task earliest start a_j and latest end b_j ; remaining instance specifics (covariate definitions, exact task counts, and resource limits) follow Mandi et al. (2024). This benchmark uses chronological train/test splits over days rather than freshly sampled Gaussian contexts.

Optimization oracles. All four oracles are solved exactly: top- k by sorting predicted item costs, shortest path and combinatorial pricing by dynamic programming, and energy scheduling as a mixed-integer program with Gurobi.

Feedback modes. All four benchmarks support pure bandit, semi-bandit, and full-information feedback in the cost-vector representation $c_t \in \mathbb{R}^{d_w}$ that matches Assumption 1. The three feedback modes share the same (H, e, d_w) across benchmarks: pure bandit reveals the scalar realized cost

$v_t = c_t^\top w_t$ via $H(w) = w^\top$, $e(w) = 1$, $d_v = 1$; semi-bandit reveals $v_t = \text{diag}(w_t) c_t$, the cost contribution of each action-selected coordinate, via $H(w) = \text{diag}(w)$, $e(w) = \mathbf{1}$, $d_v = d_w$; full information reveals $v_t = c_t$ via $H(w) = I$, $e(w) = w$, $d_v = d_w$. What differs across benchmarks is only what each coordinate of c_t represents: per-item costs (top- k), per-edge costs (shortest path), per-(product, price-level) realized demand contributions (pricing), and per-(task, machine, start-slot) energy costs (energy). On the energy benchmark, semi-bandit feedback exposes these per-(task, machine, start-slot) entries of the lifted c_t , not the original 48-slot price profile.

G Baseline algorithms

The contextual-bandit baselines below use the same pure bandit feedback $v_t = c_t^\top w_t$ as Algorithm 1. GreedyCB exploits a point prediction, ϵ -GreedyCB replaces that point prediction by a standard-normal random cost vector on exploration iterations (default $\epsilon = 0.1$), and TSCB samples from the learned conditional cost distribution.

Algorithm 2: Greedy contextual bandit (GREEDYCB)

Input: Initial parameters $\theta_1 \in \mathbb{R}^{d_\theta}$; stepsize $\eta_t > 0$
for $t = 1, 2, \dots, T$ **do**
 Observe context x_t ;
 Commit to $w_t \in \arg \min_{w \in \mathcal{S}} f_{\theta_t}(x_t)^\top w$;
 Observe feedback v_t ;
 $L_t^G(\theta) \leftarrow (f_{\theta}(x_t)^\top w_t - v_t)^2$;
 $\theta_{t+1} \leftarrow \theta_t - \eta \nabla_{\theta} L_t^G(\theta)|_{\theta=\theta_t}$;
end

Algorithm 3: ϵ -Greedy contextual bandit (ϵ -GREEDYCB)

Input: Initial parameters $\theta_1 \in \mathbb{R}^{d_\theta}$; stepsize $\eta > 0$; exploration probability $\epsilon \in [0, 1]$
for $t = 1, 2, \dots, T$ **do**
 Observe context x_t ;
 Draw $U_t \sim \text{Unif}[0, 1]$;
 if $U_t \leq \epsilon$ **then**
 Sample a random exploratory cost vector $\xi_t \sim \mathcal{N}(0, I_d)$;
 $\tilde{c}_t \leftarrow \xi_t$;
 else
 $\tilde{c}_t \leftarrow f_{\theta_t}(x_t)$;
 end
 Commit to $w_t \in \arg \min_{w \in \mathcal{S}} \tilde{c}_t^\top w$;
 Observe feedback v_t ;
 $L_t^{\epsilon-G}(\theta) \leftarrow (f_{\theta}(x_t)^\top w_t - v_t)^2$;
 $\theta_{t+1} \leftarrow \theta_t - \eta \nabla_{\theta} L_t^{\epsilon-G}(\theta)|_{\theta=\theta_t}$;
end

Algorithm 4: Thompson-style contextual bandit (TSCB)

Input: Initial parameters $\theta_1 \in \mathbb{R}^{d_\theta}$ of a conditional distribution $p_\theta(\cdot | x)$; stepsize $\eta > 0$
for $t = 1, 2, \dots, T$ **do**
 Observe context x_t ;
 Sample $\hat{c}_t \sim p_{\theta_t}(\cdot | x_t)$;
 Commit to $w_t \in \arg \min_{w \in \mathcal{S}} \hat{c}_t^\top w$;
 Observe feedback v_t ;
 Let $q_\theta(\cdot | x_t, w_t)$ be the distribution of $c^\top w_t$ induced by $c \sim p_\theta(\cdot | x_t)$;
 $L_t^{\text{TS}}(\theta) \leftarrow -\log q_\theta(v_t | x_t, w_t)$;
 $\theta_{t+1} \leftarrow \theta_t - \eta \nabla_{\theta} L_t^{\text{TS}}(\theta)$;
end

Semi-bandit adaptation. Under semi-bandit feedback, the CB baselines retain their action-selection rules but replace the scalar squared-loss update by the vector form $\|v_t - H(w_t) f_\theta(x_t)\|^2$, i.e., the same nuisance least-squares objective minimized by f_ϕ in Algorithm 1, applied to the CB cost predictor. For coordinate-mask observations $H(w_t) = \text{diag}(w_t)$ this reduces to a per-coordinate masked regression on the action-selected entries. CB learning rates are not retuned for semi-bandit; the comparison reflects identical CB policies fed a richer supervised signal.

H Generative parameterizations

Conditional normalizing-flow score function. For a conditional normalizing flow with tractable density $p_\theta(\cdot | x)$, the score function gradient uses the exact log-density,

$$g_{t,\text{CNF}}^{\text{score}} = y_t \nabla_\theta \log p_{\theta_t}(\hat{c}_t | x_t),$$

Conditional diffusion score function. For a conditional diffusion model $p_\theta(\cdot | x)$, the log-density is intractable, so the score function gradient is approximated using an ELBO proxy $\mathcal{B}_\theta(c, x)$ for $\log p_\theta(c | x)$ (Ho et al., 2020),

$$g_{t,\text{diff}}^{\text{score}} = y_t \nabla_\theta \mathcal{B}_{\theta_t}(\hat{c}_t, x_t),$$

Because \mathcal{B}_θ is a biased proxy for $\log p_\theta$, the diffusion variant falls outside Theorem 2.3’s coverage and is reported as an empirical extension; the diffusion configurations in Appendix L.2 use $\alpha_{\max} = \alpha_{\min} = 0$ to deactivate the score function path in practice.

Plug-in/surrogate-gradient variants for generative cost models. Both generative parameterizations admit the same plug-in/surrogate-gradient construction. At iteration t , sample K cost scenarios from the policy,

$$\hat{c}_t^{(1)}, \dots, \hat{c}_t^{(K)} \sim p_{\theta_t}(\cdot | x_t), \quad \bar{c}_t := \frac{1}{K} \sum_{k=1}^K \hat{c}_t^{(k)},$$

and let $g_{\text{loss}}(\hat{c}, f_\phi(x))$ denote the analytical plug-in/surrogate gradient at predicted cost \hat{c} and nuisance estimate $f_\phi(x)$. We use two variants, defined as surrogate losses whose gradient with respect to θ flows only through the reparameterized samples $\hat{c}_t^{(k)}(\theta)$ and $\bar{c}_t(\theta)$, with g_{loss} evaluated at the current iterate.

Per-scenario gradient variant. Evaluate the surrogate gradient separately for each generated scenario and average,

$$g_t^{\text{ps}} = \frac{1}{K} \sum_{k=1}^K g_{\text{loss}}(\hat{c}_t^{(k)}, f_{\phi_t}(x_t)), \quad L_t^{\text{ps}}(\theta) = \frac{1}{K} \sum_{k=1}^K \langle \hat{c}_t^{(k)}(\theta), g_t^{\text{ps}} \rangle.$$

For oracle-call point surrogates, this requires K surrogate evaluations.

Sample-average approximation (SAA) variant. Average scenarios first, then evaluate the surrogate gradient once at the empirical mean,

$$g_t^{\text{SAA}} = g_{\text{loss}}(\bar{c}_t, f_{\phi_t}(x_t)), \quad L_t^{\text{SAA}}(\theta) = \langle \bar{c}_t(\theta), g_t^{\text{SAA}} \rangle.$$

For oracle-call point surrogates, SAA requires a single surrogate evaluation rather than K .

The two variants give the same gradient only when $g_{\text{loss}}(\bar{c}_t, f_{\phi_t}(x_t)) = \frac{1}{K} \sum_{k=1}^K g_{\text{loss}}(\hat{c}_t^{(k)}, f_{\phi_t}(x_t))$, for example when the surrogate gradient is affine in the predicted cost or independent of it after fixing the candidate pool. For oracle-call losses such as SPO+, DBB, PG, IMLE, and PFYL, this need not hold because the oracle solution can change with the predicted cost.

Hybrid policy update for the diffusion parameterization. With auxiliary plug-in $g_t^{\text{aux}} \in \{g_t^{\text{ps}}, g_t^{\text{SAA}}\}$ and the simple (unweighted) denoising-MSE regularizer

$$g_t^{\text{reg}} = \nabla_\theta \mathbb{E}_{\tau, \varepsilon} \left[\|\varepsilon - \varepsilon_{\theta_t}(\hat{c}_t^{(\tau)}, \tau, x_t)\|^2 \right],$$

where $\tilde{c}_t \sim p_{\theta_t}(\cdot | x_t)$ and $\tilde{c}_t^{(\tau)}$ is its forward-noised version at diffusion step τ , the hybrid policy update is

$$g_t^{\alpha_t} = \alpha_t g_{t,\text{diff}}^{\text{score}} + (1 - \alpha_t) \left[\kappa_{\text{diff}} g_t^{\text{aux}} + \lambda_{\text{reg}} g_t^{\text{reg}} \right].$$

The hyperparameters κ_{diff} and λ_{reg} are tuned per setting (Appendix L.2).

Without the $\lambda_{\text{reg}} g_t^{\text{reg}}$ term, the auxiliary surrogate alone does not anchor the generated scenarios to the conditional density of the true cost: gradients can drift the actor into low-entropy or off-distribution regions that minimize g_t^{aux} locally without preserving the meaning of $\tilde{c}_t \sim p_{\theta_t}(\cdot | x_t)$.

I Score function variance-reduction baselines

The score function component in Algorithm 1 uses the realized scalar feedback v_t as the weight on $\nabla_{\theta} \log p_{\theta_t}(\hat{c}_t | x_t)$. In experiments we replace v_t with $v_t - b_t$ for some baseline b_t ,

$$g_t^{\text{score}} = (v_t - b_t) \nabla_{\theta} \log p_{\theta_t}(\hat{c}_t | x_t),$$

which preserves unbiasedness whenever b_t is independent of \hat{c}_t given x_t and typically reduces variance. We consider two baselines.

Moving-average baseline. A scalar running average of past feedback. Initialize $\bar{v}_0 = 0$ and update

$$b_t^{\text{ma}} = \bar{v}_t, \quad \bar{v}_{t+1} = \psi \bar{v}_t + (1 - \psi) v_t,$$

with default momentum $\psi = 0.95$. This baseline is zero-cost and never noisier than v_t itself, but ignores the context x_t .

Nuisance-induced baseline. A context-dependent baseline computed from the nuisance estimate. Let

$$w_t^{\phi} := w^*(f_{\phi_t}(x_t)) \in \arg \min_{w \in \mathcal{S}} f_{\phi_t}(x_t)^{\top} w$$

denote the nuisance-induced optimal decision, and define

$$b_t^{\text{ni}} = f_{\phi_t}(x_t)^{\top} w_t^{\phi},$$

the nuisance’s own predicted optimum at x_t . When the implemented decision w_t matches w_t^{ϕ} , the gradient weight $v_t - b_t^{\text{ni}}$ collapses to the residual $v_t - f_{\phi_t}(x_t)^{\top} w_t$; when w_t is worse than w_t^{ϕ} under the nuisance, the weight is positive, so the gradient descent step reduces the probability of generating \hat{c}_t . This choice uses the context but adds one oracle solve per iteration. Since b_t^{ni} depends only on x_t and past data, a miscalibrated nuisance affects the variance of the score function gradient but not its unbiasedness.

J Adaptive mixing-weight schedule

Algorithm 1 treats the mixing parameter α as a fixed scalar; in our experiments we instead use a time-varying α_t , applied in the hybrid gradient $g_t^{\alpha_t} = \alpha_t g_t^{\text{score}} + (1 - \alpha_t) g_t^{\text{plug-in}}$ (and analogously with g_t^{sur} in the surrogate variant). The schedule decays α_t from α_{max} toward α_{min} , weighting the unbiased score function gradient more heavily early on (when the nuisance estimate is unreliable) and the lower-variance plug-in gradient later (as the nuisance estimate stabilizes). We use two variants that differ only in how the decay is gated. Both gates are specified in absolute iterations rather than as a fraction of T to avoid leaking the horizon into the schedule.

Fixed-warmup variant. For the first T_{warm} iterations (default $T_{\text{warm}} = 100$), the target is held at $\alpha_t^* = \alpha_{\text{max}}$; afterwards $\alpha_t^* = \alpha_{\text{min}}$.

Exponential-gate variant. Used in focused generative-model tuning. The target blends α_{max} and α_{min} via an exponentially decaying weight,

$$g_t = \exp(-(t - 1)/\tau_{\text{sched}}), \quad \alpha_t^* = g_t \alpha_{\text{max}} + (1 - g_t) \alpha_{\text{min}},$$

where τ_{sched} controls the decay timescale (smaller τ_{sched} moves to the α_{min} regime faster).

Smoothed update. In both variants, the actual mixing weight applies smoothing with rate η_α (default 0.05) and re-clips,

$$\alpha_t = \text{clip}((1 - \eta_\alpha) \alpha_{t-1} + \eta_\alpha \alpha_t^*, \alpha_{\min}, \alpha_{\max}).$$

Remark. Both variants use α_{\min} as a fixed post-warmup target. More adaptive heuristics are straightforward to substitute: for example, α_{\min} can be replaced by a reliability-driven target that responds to the running prediction error of the nuisance estimate (so that α_t rises again whenever the nuisance loses accuracy).

K Additional experimental results

This section collects supplementary tables and figures for the numerical study. The main text reports the headline comparisons; the appendix gives convergence plots, sensitivity analyses, and the feedback-mode comparison. Compute resources used to run the experiments are reported in Appendix M.

K.1 Convergence plots

The main text reports the top- k convergence plot. Figure 3 gives the corresponding shortest-path, pricing, and real-data energy-scheduling trajectories, zoomed into the first 600 iterations of the $T = 2,000$ run for the synthetic benchmarks. On shortest path, all methods pay for the noisy first iterations, but the hybrid curve settles below the contextual-bandit baselines and remains the lowest curve through the later part of this window. On pricing, after a short transient, DFHPG and DFHPG-0 separate from the rest of the methods and continue to reduce average regret, while DFHPG-1 behaves much more like the contextual-bandit baselines, indicating that the scalar revenue feedback alone is not enough to recover the useful price structure and the decision-focused surrogate supplies most of the useful direction.

K.2 Distributional cost models on the remaining benchmarks

The main text (Figure 2) compares distributional cost models – Gaussian linear, CNF, and diffusion – on pricing at the extended horizon $T = 15,000$. Figure 4 reports the same comparison on the three remaining benchmarks: top- k selection, shortest path, and energy scheduling. The synthetic benchmarks use $T = 15,000$; the energy benchmark uses its native test-window length.

On top- k selection and shortest path, the ranking from pricing carries over: the Gaussian linear model leads early, while CNF closes the gap and reaches the lowest final regret. Diffusion trails throughout; one possible factor is the ELBO-based approximation that replaces an exact log-density. On the energy-scheduling benchmark, the differences across distributional cost models are within run-to-run variability, which we attribute to the low-signal real-data regime already noted in the main text.

K.3 Surrogate-loss definitions

We follow the gradient form of each surrogate from the reference implementations of PyEPO (Tang and Khalil, 2024); pool-based variants follow the cumulative-pool formulation of the PredOpt-Benchmarks suite of Mandi et al. (2024). Throughout, \hat{c} is the predicted cost vector, c the target cost (the true cost in offline DFL; the nuisance estimate $f_\phi(x)$ in our hybrid plug-in update), $w^*(\cdot) \in \arg \min_{w \in \mathcal{S}} (\cdot)^\top w$ the linear-optimization oracle, $w_{\text{ptb}}^*(c) := \mathbb{E}_\xi [w^*(c + \sigma\xi)]$ a perturbed-oracle expectation with $\xi \sim \mathcal{N}(0, I)$, and $\mathcal{L}_{\text{task}}(w; c) = c^\top w$ the regret-style task loss. All subgradients below are stated with respect to \hat{c} in the cost-minimization convention; the parameter update applies $\hat{c} \leftarrow \hat{c} - \eta \nabla_{\hat{c}} \ell^{\text{sur}}$.

Oracle-call surrogates. These call w^* once or twice per gradient evaluation.

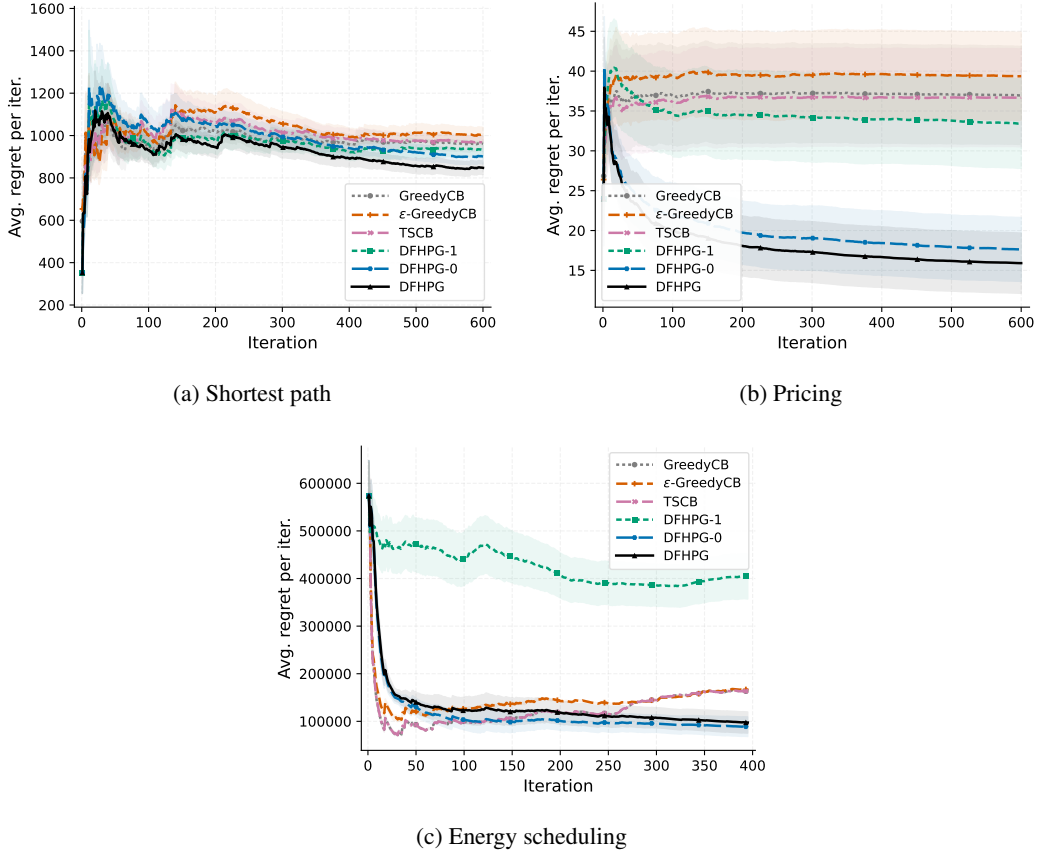


Figure 3: Convergence plots for shortest path, pricing, and energy scheduling. Synthetic benchmarks are zoomed to the first 600 iterations; the energy benchmark uses its native test-window length. Each curve reports average regret per iteration, with shaded ± 1 standard-error bands across replications.

Loss	Subgradient $\nabla_{\hat{c}} \ell^{\text{sur}}(\hat{c}, c)$
SPO+ (Elmachtoub and Grigas, 2022)	$2(w^*(c) - w^*(2\hat{c} - c))$
MSE+SPO+	$\beta_{\text{mse}}(\hat{c} - c) + (1 - \beta_{\text{mse}}) \nabla_{\hat{c}} \ell_{\text{SPO+}}$
DBB (Vlastelica et al., 2020)	$(w^*(\hat{c}) - w^*(\hat{c} + \lambda_{\text{ptb}}c)) / \lambda_{\text{ptb}}$
IMLE (Niepert et al., 2021)	$(w_{\text{ptb}}^*(\hat{c}) - w_{\text{ptb}}^*(\hat{c} + \lambda_{\text{ptb}}c)) / \lambda_{\text{ptb}}$
AIMLE (Minervini et al., 2023)	IMLE with adaptive $\lambda_{\text{ptb}} = \alpha \ \hat{c}\ / \ c\ $, α updated by EMA on grad sparsity
NID (Sahoo et al., 2023)	$-c$ (negative-identity straight-through)
PFYL (Berthet et al., 2020)	$\bar{w}_{\text{ptb}}^*(\hat{c}) - w^*(c)$
DPO (Berthet et al., 2020)	$\frac{1}{M\sigma} \sum_{i=1}^M \xi_i \langle w^*(\hat{c} + \sigma \xi_i), c \rangle$, $\xi_i \sim \mathcal{N}(0, I)$
PG (Gupta and Huang, 2024)	$(w^*(\hat{c} - \sigma c) - w^*(\hat{c})) / \sigma$

Pool-based surrogates. Let \mathcal{P}_t denote the cumulative pool of feasible solutions at iteration t , grown online by appending $w^*(\hat{c}_t)$ and $w^*(c_t)$ at each step. Let $w_b := \arg \min_{w \in \mathcal{P}_t} c^\top w$ denote the pool's best solution under the target cost and $\mathcal{R}_t := \mathcal{P}_t \setminus \{w_b\}$ the rest of the pool; let $\delta > 0$ be the LTR margin and $\tau_{1w} > 0$ the listwise temperature.

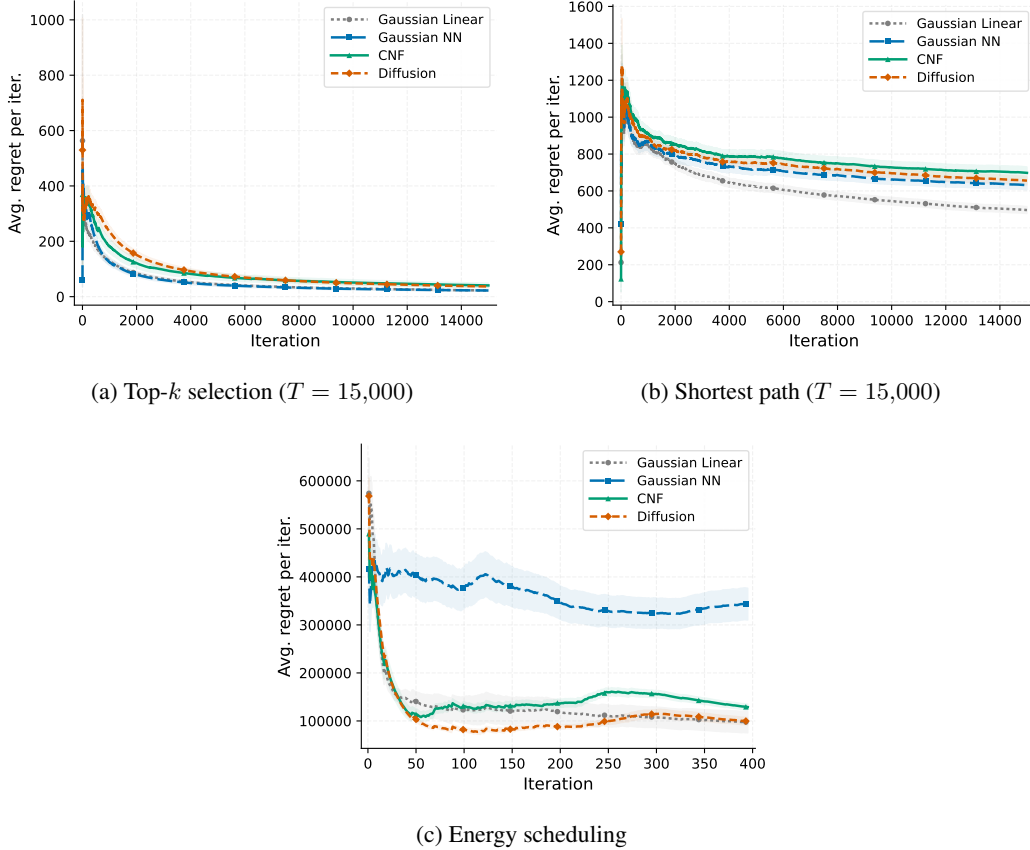


Figure 4: Comparison of distributional cost models on top- k selection, shortest path, and energy scheduling. Each curve reports average regret per iteration, with shaded ± 1 standard-error bands across replications.

Loss	Subgradient $\nabla_{\hat{c}} \ell^{\text{sur}}(\hat{c}, c)$
NCE (Mulamba et al., 2021)	$w^*(c) - \frac{1}{ \mathcal{P}_t } \sum_{w \in \mathcal{P}_t} w$
contrastiveMAP (Mulamba et al., 2021)	$w^*(c) - \arg \min_{w \in \mathcal{P}_t} \hat{c}^\top w$
pointwiseLTR (Mandi et al., 2022)	$\frac{2}{ \mathcal{P}_t } \sum_{w \in \mathcal{P}_t} ((\hat{c} - c)^\top w) w$
pairwiseDiff (Mandi et al., 2022)	$\frac{2}{ \mathcal{R}_t } \sum_{r \in \mathcal{R}_t} \Delta_{br}(w_b - w_r), \Delta_{br} = (\hat{c} - c)^\top (w_b - w_r)$
pairwiseLTR (Mandi et al., 2022)	$\sum_{r \in \mathcal{R}_t: \hat{c}^\top w_b > \hat{c}^\top w_r - \delta} (w_b - w_r)$ (max-margin hinge)
listwiseLTR (Mandi et al., 2022)	$\frac{1}{\tau_{1w}} (\sigma_{\text{soft}}(-\hat{c}^\top \mathcal{P}_t / \tau_{1w}) - \sigma_{\text{soft}}(-c^\top \mathcal{P}_t / \tau_{1w})) \mathcal{P}_t$
NCE_c (Mulamba et al., 2021)	Same subgradient as NCE; cached/centered pool variant
MAP_c (MAP-C) (Mulamba et al., 2021)	$w^*(c) - \arg \min_{w \in \mathcal{P}_t} (\hat{c} - c)^\top w$ (cached MAP variant)
SPOCaching (Mulamba et al., 2021)	$\arg \min_{w \in \mathcal{P}_t} (2\hat{c} - c)^\top w - w^*(c)$

Here σ_{soft} denotes softmax and $\hat{c}^\top \mathcal{P}_t \in \mathbb{R}^{|\mathcal{P}_t|}$ stacks the predicted-cost utilities of pool entries. The negative signs on the softmax arguments convert cost minimization to score maximization for the listwise ranking step. The heatmaps use implementation labels: SPOPlus and MSE+SPOPlus correspond to the SPO+ and MSE+SPO+ rows above, and MAP-C is the selected-configuration spelling of MAP_c.

Use in the hybrid update. With the reparameterization $\hat{c} = \mu_\theta(x, \varepsilon)$ of Assumption 4, any surrogate above enters the policy parameters via the chain rule $g_t^{\text{sur}} = (\nabla_\theta \mu_\theta(x_t, \varepsilon_t))^\top \nabla_{\hat{c}} \ell^{\text{sur}}(\hat{c}_t, f_{\phi_t}(x_t))$, i.e., the nuisance estimate $f_\phi(x)$ supplies the target cost c in each formula above. Theorem 2.3 covers the convergence of the resulting hybrid update for any surrogate whose subgradient satisfies the regularity bounds of Assumption 9.

K.4 Alternative surrogate choices

The surrogate loss for the decision-focused plug-in component is treated as a tunable hyperparameter rather than fixed to a default. This appendix reports the per-benchmark sweep over standard surrogate choices, implemented following the PyEPO reference implementations (Tang and Khalil, 2024), across the pricing, shortest-path, top- k , and energy-scheduling benchmarks. All synthetic comparisons in this section use the Gaussian linear cost model; the energy comparison uses the same setup as in the main results. Each heatmap changes only the surrogate loss used by the decision-focused component; the score function update, nuisance update, contexts, feasible set, and feedback model are held fixed. The two columns correspond to the full hybrid update DFHPG and the plug-in-only update DFHPG-0. Cell values are mean final cumulative regret, so lower values are better.

Figure 5 shows that no single surrogate dominates across benchmarks, motivating the per-problem tuning protocol. On pricing, contrastive and ranking-style losses (contrastiveMAP, DBB, pairwiseDiff, listwiseLTR) lead in both columns, while NID and MSE+SPOPlus trail. On shortest path, DFHPG is approximately flat across a wide best group (AIMLE, pairwiseDiff, NID, DPO, PFYL, PG), whereas DFHPG-0 is more variable and peaks at SPOPlus, SPOCaching, and AIMLE. On top- k selection, NID, pairwiseDiff, and MSE+SPOPlus lead for DFHPG, while DFHPG-0 prefers NID and SPO-type losses. On energy scheduling the ranking inverts relative to pricing: pairwiseDiff, MSE+SPOPlus, IMLE, and NCE lead, while DBB and contrastiveMAP, the pricing winners, fall to the bottom half, and PG and DPO collapse by an order of magnitude. Across all four problems, DFHPG is consistently no more sensitive to surrogate choice than DFHPG-0: the hybrid update partially absorbs a poor surrogate through the score function component.

K.5 Mixing-weight sensitivity

Figure 6 ablates the mixing weight between the score function and plug-in components. We compare the adaptive schedule from Appendix J against fixed values of α on all four benchmarks. The adaptive schedule is a strong default but does not strictly dominate the best fixed α : on top- k selection, shortest path, and pricing it matches or modestly improves on the strongest fixed setting, validating the early-score / late-plug-in transition; on the energy-scheduling benchmark it trails the smaller fixed α values, consistent with the score function gradient being uninformative in this low-signal real-data regime, where any positive weight on the score component hurts.

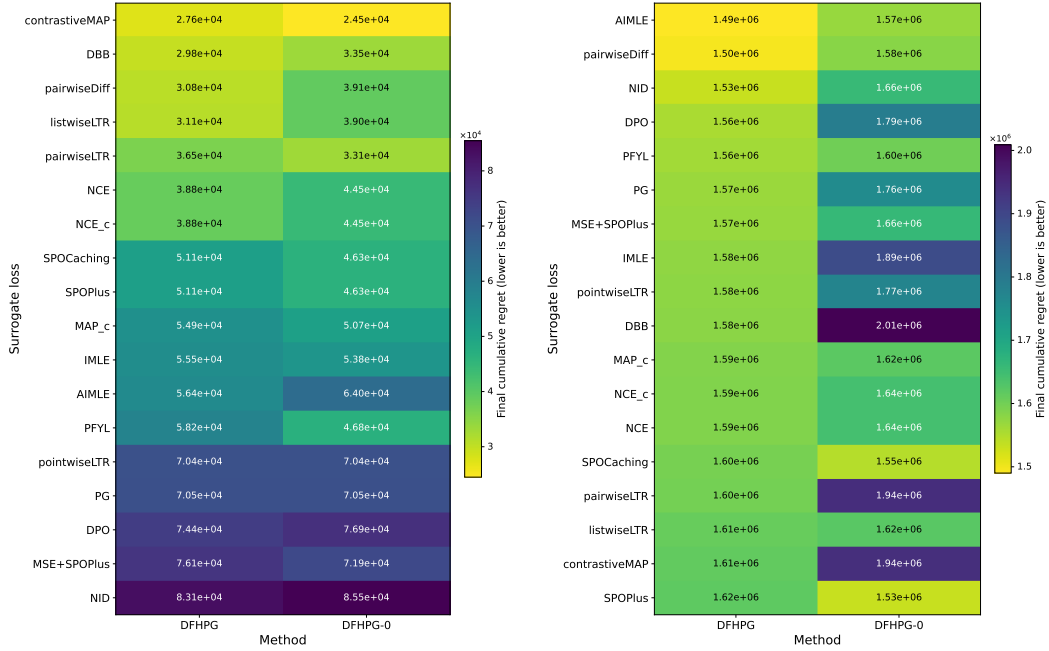
K.6 Sensitivity across problem difficulty

Figure 7 reports degree-robustness on pricing, shortest path, and top- k selection, where the polynomial degree controls the nonlinearity of the synthetic cost generator (top- k and shortest path) or the demand generator (pricing). Higher degrees act as a difficulty knob: every method’s regret rises monotonically with degree, confirming that the problem itself becomes harder to learn under the Gaussian linear cost model used in this comparison. Across degrees, DFHPG and DFHPG-0 retain a regret advantage over the contextual-bandit baselines, but the magnitude of the gap is benchmark-specific. On pricing the gap is largest at low degrees (over an order of magnitude at $\text{deg} = 2$) and narrows at high degrees, where the Gaussian linear cost model can no longer capture the cost map well. On top- k the gap is more modest at low degrees (around $2\times$ at $\text{deg} = 2$) and widens to roughly $4\text{--}5\times$ at $\text{deg} \geq 4$. Shortest path shows small gaps throughout. The score-only DFHPG-1 ablation largely tracks the baselines, indicating that the decision-focused plug-in component is what drives the advantage as the problem hardens.

K.7 Feedback mode comparison

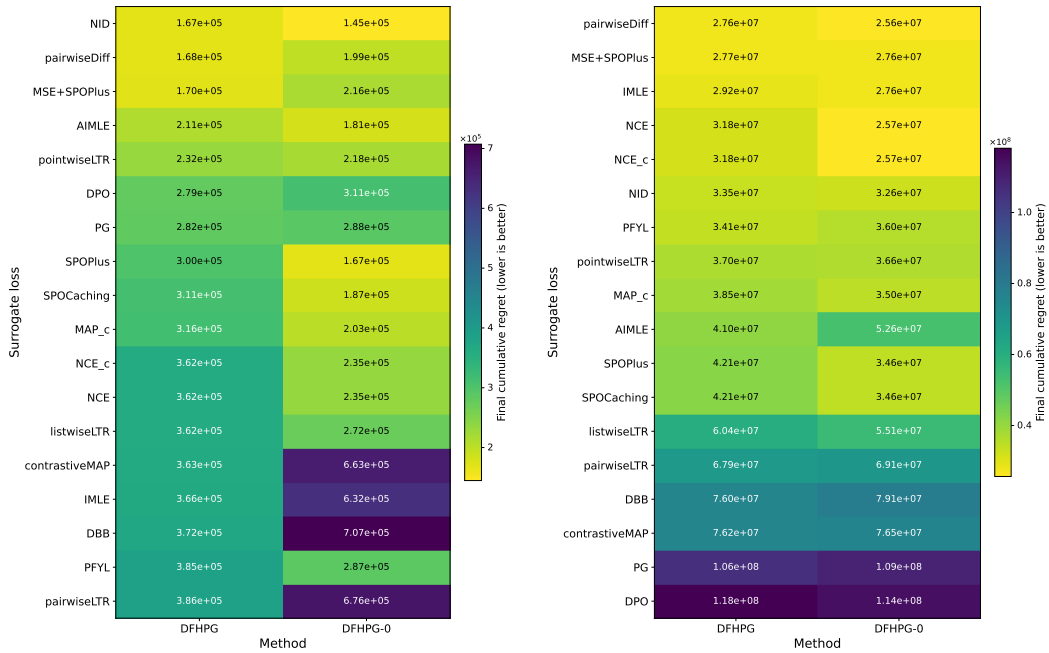
Figure 8 compares final cumulative regret across three feedback modes (pure bandit, semi-bandit, and full information) for both DFHPG and DFHPG-0 on each benchmark. The pattern is consistent across all four problems: regret decreases monotonically as feedback becomes richer, since stronger feedback either accelerates the nuisance estimator or replaces it with full observation. On the energy benchmark the variance contraction is especially large, with pure-bandit error bars roughly an order of magnitude wider than under semi-bandit or full feedback.

Table 2 reports final cumulative regret under semi-bandit feedback for the contextual-bandit baselines and DFHPG variants. The CB baselines use the semi-bandit-adapted regression update described



(a) Pricing

(b) Shortest path



(c) Top- k selection

(d) Energy scheduling

Figure 5: Surrogate-loss comparison across the four benchmark problems. Each heatmap reports mean final cumulative regret for DFHPG and DFHPG-0 when changing only the surrogate loss used by the decision-focused component; lower values are better.

at the end of Appendix G; their action-selection rules are unchanged. DFHPG-0 is best on every benchmark; the closest CB baseline (TSCB on pricing) still trails by roughly $2\times$.

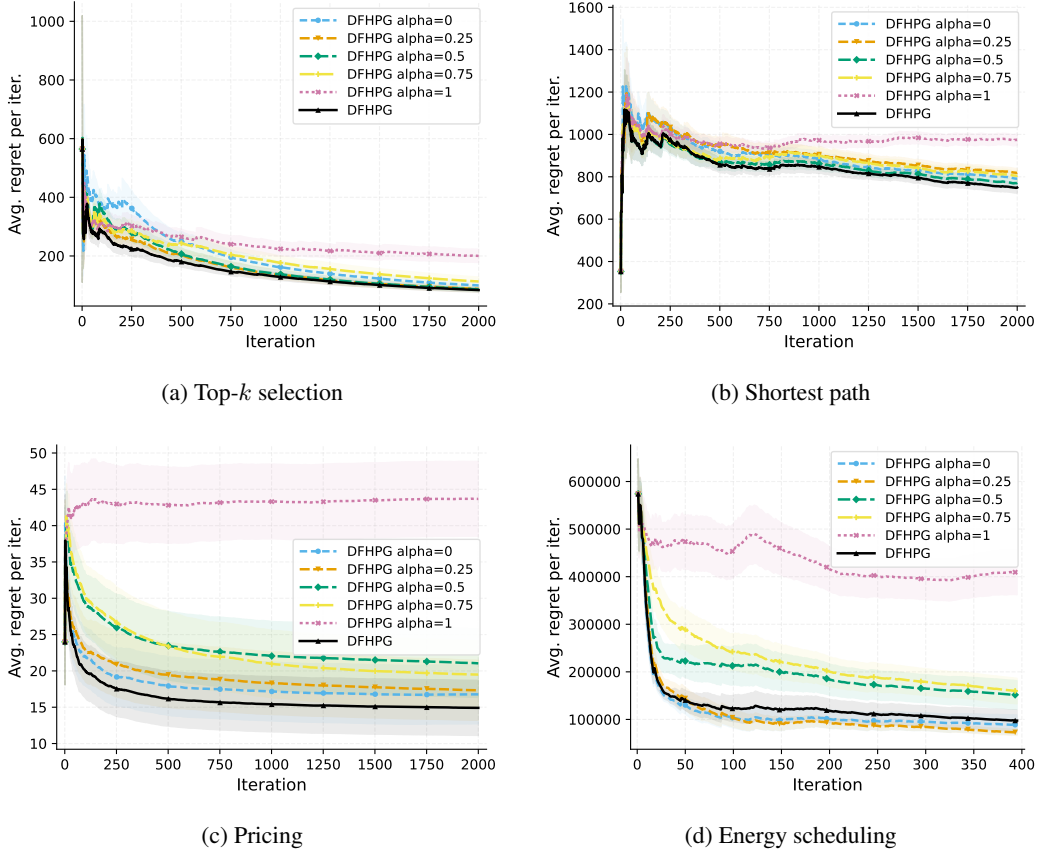


Figure 6: Mixing-weight ablation comparing the adaptive α_t schedule against fixed α on the four benchmarks. Each curve reports average regret per iteration, with shaded ± 1 standard-error bands across replications.

Table 2: Final cumulative regret under semi-bandit feedback. The contextual-bandit baselines use the semi-bandit-adapted regression update of Appendix G. Setup matches Table 1; the best result in each column is bolded.

Method	Top- k (deg. 8)	Shortest path (deg. 8)	Pricing (deg. 8)	Energy
GREEDYCB	$3.01 \times 10^5 \pm 1.61 \times 10^4$	$9.37 \times 10^5 \pm 2.32 \times 10^4$	$3.48 \times 10^4 \pm 7.92 \times 10^3$	$2.66 \times 10^7 \pm 1.07 \times 10^5$
ϵ -GREEDYCB	$2.91 \times 10^5 \pm 2.01 \times 10^4$	$9.87 \times 10^5 \pm 3.29 \times 10^4$	$4.36 \times 10^4 \pm 7.14 \times 10^3$	$4.16 \times 10^7 \pm 4.83 \times 10^5$
TSCB	$2.87 \times 10^5 \pm 1.86 \times 10^4$	$9.67 \times 10^5 \pm 3.31 \times 10^4$	$1.47 \times 10^4 \pm 5.99 \times 10^3$	$2.66 \times 10^7 \pm 1.08 \times 10^5$
DFHPG	$7.10 \times 10^4 \pm 8.52 \times 10^3$	$6.83 \times 10^5 \pm 3.11 \times 10^4$	$7.54 \times 10^3 \pm 5.86 \times 10^2$	$2.35 \times 10^7 \pm 4.21 \times 10^5$
DFHPG-0	$6.65 \times 10^4 \pm 5.30 \times 10^3$	$5.31 \times 10^5 \pm 2.28 \times 10^4$	$7.30 \times 10^3 \pm 6.46 \times 10^2$	$2.33 \times 10^7 \pm 3.78 \times 10^5$

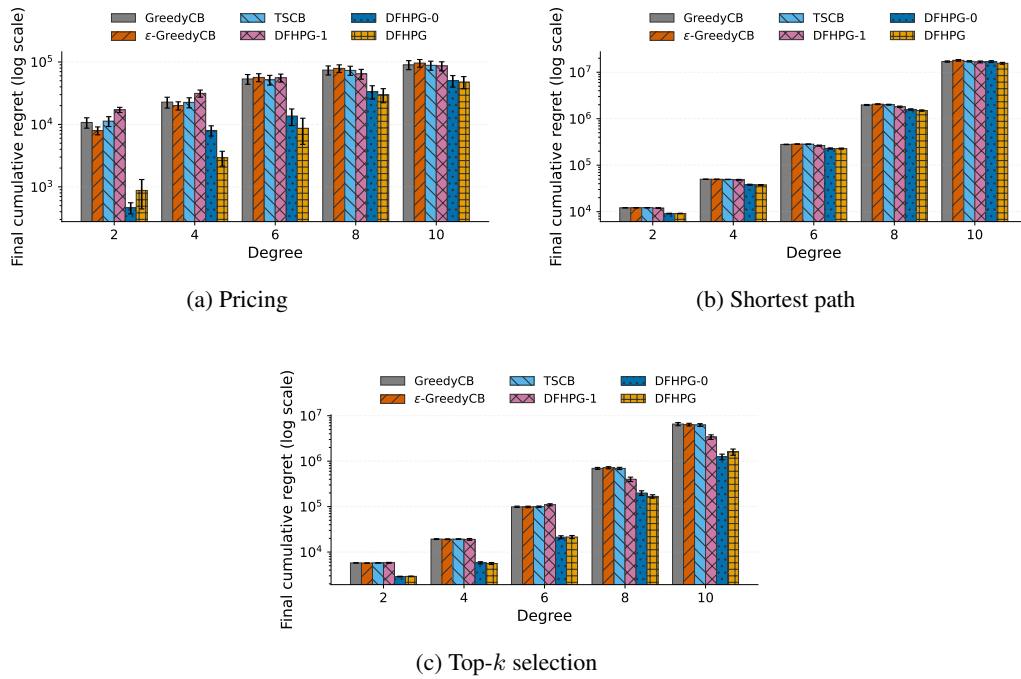


Figure 7: Sensitivity across problem difficulty under moderate noise for pricing, shortest path, and top- k selection. Each plot compares final cumulative regret across polynomial degrees for the Gaussian linear cost-model experiments. Lower is better.

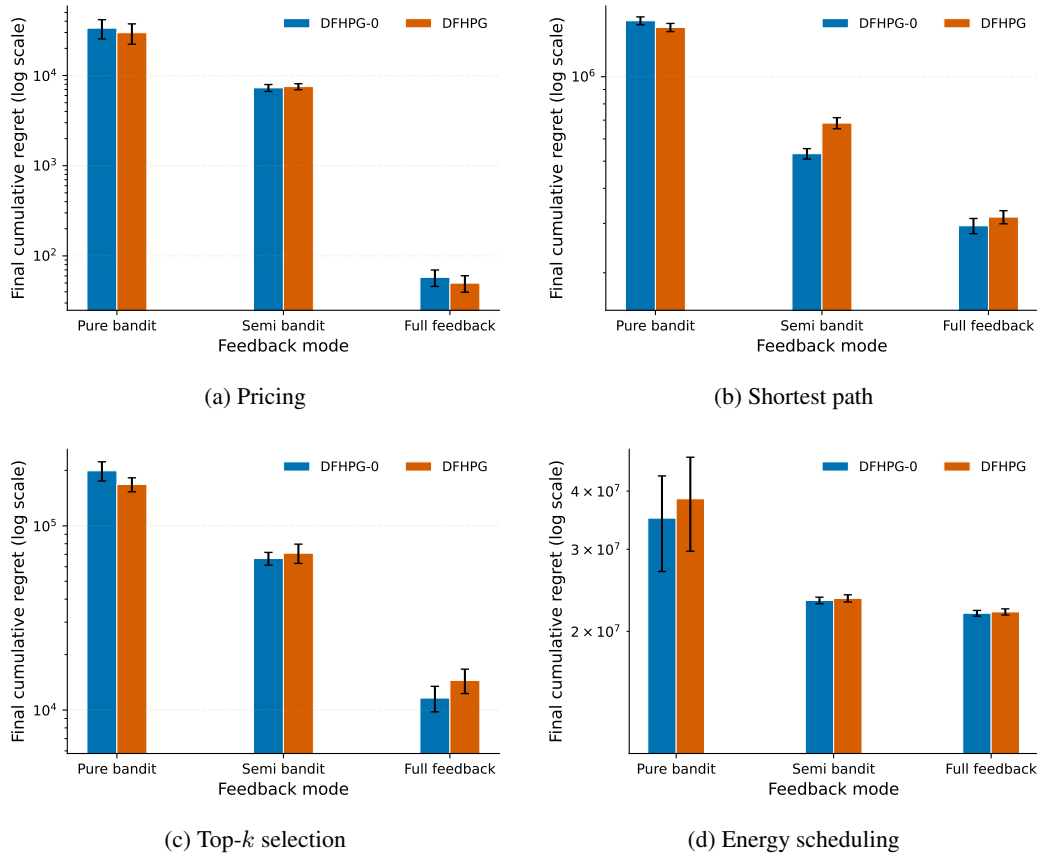


Figure 8: Feedback mode comparison across the four benchmarks. Each plot compares final cumulative regret across feedback modes (bandit, semi-bandit, full information) on a log-scaled regret axis. Synthetic panels use the Gaussian linear cost-model experiments. Lower is better.

L Hyperparameter selection

L.1 Tuning protocol

Hyperparameters were selected by random search per (benchmark, distributional cost model) on dedicated validation runs that share no seeds with the reported paper runs. Validation used 10 seeds for top- k , shortest path, and pricing, and 5 seeds for energy; the paper results use 30 seeds. Validation horizons were $T = 2,000$ for the point-model sweep, $T = 5,000$ for a two-stage generative screen, and $T = 394$ on the energy load3 split (validation fraction 0.5); paper horizons are $T = 2,000$ for point models, $T = 15,000$ for the generative comparison, and the held-out experiment split for energy. Candidates were ranked by mean final cumulative regret on the validation seeds. Full search spaces and per-benchmark sweep specifications are available in the supplementary code.

L.2 Selected configurations

Across (benchmark, distributional cost model) settings, the selected configurations share the following defaults:

- Policy and nuisance learning rates on the same shifted-inverse schedule, $\eta^t = \eta^0 / (1 + t/o)$ with offset $o = 100$. The reported η_θ^0 and η_ϕ^0 are the initial values.
- Adaptive mixing-weight schedule (Appendix J): EMA decay 0.98 on the residual ratio, smoothing factor 0.05 on α_t updates, fixed-warmup gate of $T_{\text{warm}} = 100$ iterations.
- Both the score function and the plug-in (surrogate) gradients are L_2 -normalized to unit norm separately before the convex mix $\alpha g_t^{\text{score}} + (1 - \alpha) g_t^{\text{plug-in}}$, so that α controls the angular interpolation direction without being warped by the two sides' raw magnitudes.

Surrogate names follow Appendix K.4; baselines are moving-average (MA) and nuisance-induced (NI) from Appendix I.

Table 3 reports the point-model configurations across all four benchmarks. Table 4 reports the generative-model configurations across the same four benchmarks. Synthetic benchmarks use the fixed-warmup variant of the adaptive schedule with the default 100-iteration warmup; the energy benchmark uses the exponential-gate variant with time scale τ_{sched} (column " τ_{sched} "; "-" for the synthetic rows). Synthetic point-model entries use $\text{deg} = 8$; synthetic generative entries use $\text{deg} = 8$ with $T = 15,000$.

Table 3: Point-model configurations across the four benchmarks. Columns: initial policy LR η_θ^0 , initial nuisance LR η_ϕ^0 , plug-in surrogate, exploration scale σ_G , mixing bounds $\alpha_{\text{max}}, \alpha_{\text{min}}$, exponential-gate time scale τ_{sched} (energy only), baseline.

Benchmark	Class	η_θ^0	η_ϕ^0	Surrogate	σ_G	α_{max}	α_{min}	τ_{sched}	Baseline
Top- k	Gaussian linear	6.8e-2	5.3e-2	pairwiseDiff	8.6e-1	0.3	0.02	-	MA
Top- k	Gaussian NN	7.5e-2	1.1e-2	IMLE	2.6e-1	0.1	0.05	-	MA
Shortest path	Gaussian linear	3.0e-2	1.5e-2	pairwiseDiff	3.9e-1	0.5	0.05	-	NI
Shortest path	Gaussian NN	3.0e-2	1.0e-2	pairwiseDiff	5.3e-1	0.3	0.02	-	NI
Pricing	Gaussian linear	9.9e-3	4.9e-3	DBB	1.1e-4	0.2	0.01	-	NI
Pricing	Gaussian NN	6.4e-3	4.5e-3	SPO+	4.8e-6	0.2	0.01	-	NI
Energy	Gaussian linear	5.0e-3	2.5e-2	MAP-C	1.9e-3	0.1	0.0	100	NI
Energy	Gaussian NN	1.0e-3	1.0e-3	DBB	5.0e-3	0.8	0.2	100	MA

The pricing-diffusion and energy-diffusion entries use $\alpha_{\text{max}} = \alpha_{\text{min}} = 0$ (plug-in only), consistent with Appendix K.5.

M Compute resources

All experiments ran on a shared HPC cluster running Red Hat Enterprise Linux 9.6. Each CPU trial uses one Intel Xeon Gold 6226 core at 2.70 GHz with 2 GB of RAM. GPU trials use a single NVIDIA L40S or RTX 6000.

Table 4: Generative-model configurations across the four benchmarks. The auxiliary plug-in path uses the per-scenario gradient (Appendix H) with surrogate as listed, K scenarios per iteration, surrogate-loss weight κ_{diff} , and generative-regularizer weight λ_{reg} . Energy CNF uses two coupling layers with hidden width 128; energy diffusion uses 20 training and 8 inference timesteps with ELBO weighting.

Benchmark	Class	η_{θ}^0	η_{ϕ}^0	α_{max}	α_{min}	τ_{sched}	Baseline	Surrogate	K	κ_{diff}	λ_{reg}
Top- k	CNF	3.0e-2	6.0e-3	0.2	0.01	–	NI	pairwiseDiff	32	3.0	1.0
Top- k	Diffusion	1.3e-2	1.3e-2	0.2	0.01	–	MA	pairwiseLTR	200	10.0	1.0
Shortest path	CNF	9.0e-3	6.8e-3	0.5	0.02	–	MA	SPO+	128	1.0	0.03
Shortest path	Diffusion	1.0e-2	1.0e-2	0.1	0.0	–	NI	pairwiseDiff	200	1.0	0.1
Pricing	CNF	3.0e-2	2.3e-2	0.2	0.01	–	NI	SPO+	200	10.0	0.3
Pricing	Diffusion	2.5e-3	2.5e-3	0.0	0.0	–	MA	SPO+	64	3.0	0.3
Energy	CNF	1.5e-2	1.1e-2	0.8	0.05	500	NI	pairwiseLTR	100	1.0	0.1
Energy	Diffusion	3.0e-3	3.0e-3	0.0	0.0	100	NI	pairwiseLTR	100	1.0	0.1